ISSN 1075-7015, Geology of Ore Deposits, 2017, Vol. 59, No. 5, pp. 354–374. © Pleiades Publishing, Ltd., 2017.
Original Russian Text © T.A. Radomskaya, O.M. Glazunov, V.N. Vlasova, L.F. Suvorova, 2017, published in Geologiya Rudnykh Mestorozhdenii, 2017, Vol. 59, No. 5, pp. 363–384.

Geochemistry and Mineralogy of Platinum Group Element in Ores of the Kingash Deposit, Eastern Sayan, Russia

T. A. Radomskaya*, O. M. Glazunov, V. N. Vlasova, and L. F. Suvorova

Institute of Geochemistry, Siberian Branch, Russian Academy of Sciences, Irkutsk, 664033 Russia

**e-mail: taniaojigova@mail.ru*

Received February 4, 2016

Abstract—The paper discusses the results of studying the contents of platinum group elements (PGE) and platinum group minerals (PGM) in ores of the Kingash deposit. The bulk of PGE has been established as concentrated in disseminated sulfide chalcopyrite–pyrrhotite–pentlandite ore and is represented by palladium bismuth–tellurides. During melt differentiation, the content and relationship of PGE are changed; the Pd/Pt value increases (up to 1.9 and 4.2 in dunite and wehrlite, respectively) with decreasing Mg number. The distribution of PGE, sulfur, and REE in various ore types suggests two formation mechanisms of high-grade ores: (1) the product of liquid immiscibility and gravity separation at the early magmatic stage and (2) involvement of the residual melt saturated in volatiles, which contributed to transportation and segregation of PGE at the late magmatic stage. The evolution of the ore system of the Kingash massif is characterized by sequential enrichment of PGM in Ni from high-Mg to low-Mg rocks similarly to sulfide minerals of disseminated ore. The criteria for ore content in utramafics of the Kansk block have been identified based on compared ore element and PGE concentrations in ultramafic rocks of the Kingash and Idar complexes.

DOI: 10.1134/S107570151705004X

INTRODUCTION

Platiniferous ultramafic–mafic complexes as a product of mantle magmatism on the Earth's surface yield valuable information about deep-seated magmatic and ore-forming processes generated by mantle plumes (Dobretsov et al., 2010; Yarmolyuk et al., 2000; Kuzmin and Yarmolyuk, 2014). The study of the crust–mantle ore-forming systems is pertinent, because platiniferous and nickel–copper ores, which are products of mantle picrite magma and indicators of the prograde stage of large igneous provinces (LIPs) (Izokh et al., 2011) are related to them. Not only central parts of LIPs, but marginal zones of ancient platforms with multiple plume magmatism are promising in this regard. One fragment of such a zone in the southern folded frame of the Siberian Platform is the Sayan Nickel–copper–PGE province (Glazunov, 1994) (Fig. 1), which was described later as part of the East Siberian metallogenic province (Polyakov et al., 2013) comprising the Kansk block, the metamorphosed sequence of which hosts ultramafic–mafic massifs. Previously referred to the single Lower Proterozoic Idar Complex, today, they are divided into the Idar restite dunite–harzburgite and Kingash cumulative dunite–wehrlite–pyroxenite–gabbro complexes.

The country rocks of ultramafic massifs are gneiss and amphibolite of two heterochronous structural complexes: (1) lower Upper Archean Karagan and (2) upper Lower Proterozoic Anzha (Nozhkin and Smagin, 1988; Nozhkin et al., 2005). They are composed of mineral assemblages pertaining to amphibolite and epidote–amphibolite facies with the following metamorphic parameters: P = 7.7–8.5 kb and T = 600–700°C (Nozhkin et al., 2001).

The Kingash Ni–Cu–PGE deposit is the single large platinum producer, which is under industrial development in southern Krasnoyarsk krai (Glazunov et al., 2003). The economic measured mineral resources of PGE, copper, and nickel (Lomaeva and Tarasov, 2010) of the Kingash dunite–wehrlite–pyroxenite–gabbro massif are related to ultramafic rocks.

Despite the heightened interest of researchers and knowledge of the petrography and mineralogy of the Kingash massif, problems related to the ore localization conditions and distribution and accumulation of precious metals and iron group elements at various stages of endogenic process are more poorly studied.

GEOLOGY AND COMPOSITION OF THE MASSIF

The Kingash massif is lopolith in plan view, consisting of dunite–wehrlite rocks overlain by gabbro. Pyroxenite is between gabbro and ultramafic rocks (Fig. 2). Minor hornblende peridotite and hornblendite were found within the massif. Dykes of plagiog-

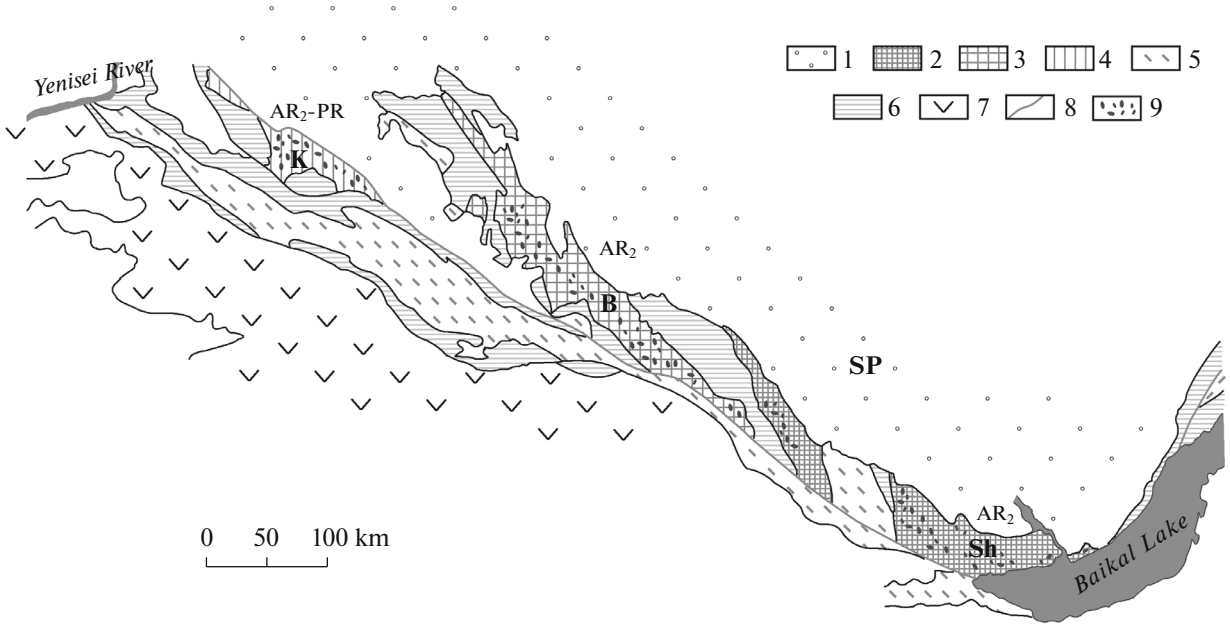

Fig. 1 Sayan Ni–Cu–PGE province within Kansk-Biryusa-Sharyzhalgai (K-B-Sh) Precambrian blocks at southern boundary of North Asia Craton (Glazunov, 2009). Tectonic basis after Sezko (1988) with materials of Altukhov et al. (1990). (1) Siberian Platform (SP); (2–4) Precambrian blocks: (2) Lower Archean Sharyzhalgain (Sh) (3.1–3.6 Ga), (3) Upper Archean Biryusa (B) (2.5-2.9 Ga), (4) Upper Archean to Proterozoic Kansk (K) (2.3–2.4 Ga); (5) Paleoproterozoic troughs and depressions; (6) Riphean–Proterozoic complex; (7) Caledonian folding area; (8) Main Sayan Lineament; (9) ultramafic–mafic massifs out of scale.

ranite and microgabbro and quartz–plagioclase veins cut the massif.

The rocks of the massif have undergone epidote–amphibolite facies metamorphism. Kingash ultramafic rocks are serpentinized, tremolitized, talcized, and carbonated to varying degrees. Unaltered ultramafic rocks are retained in the central part of the massif. They are composed of olivine and pyroxene retained to varying degrees and are cumulus. Olivine frequently contains inclusions of Cr-pleonast. Dunite graduates to wehrlite as demonstrated by the increasing content of clinopyroxene and edenite and appearance of pargasite. The content of phlogopite in ultramafic rocks is 1 vol % as usual, but in some places it reaches 5–7 vol %. Clinopyroxenite is composed of diopside, poikilitic olivine, pale brown hornblende (pargasite), and phlogopite. Gabbro is strongly altered. Plagioclase is replaced by zoisite and epidote; amphibole replaces monoclinic pyroxene. Minor titanite and mica are found.

Subtle zoning of the massif has been identified as variation in the chemical composition of coexisting silicate minerals (Fig. 3). The most significant differences in the chemical composition of these phases are between ultramafic and mafic rocks and minerals of various generations. For example, the early-generation spinel enclosed in olivine of dunite is Cr-pleonast, whereas intercumulus spinel corresponds to picrochromite. The content of the fayalite (Fa) endmember in Kingash olivine increases from 13–16% in dunite and wehrlite to 22–24% in olivine clinopyroxenite, whereas the Ni concentration decreases 0.33 wt % to trace amounts. Clinopyroxene in wehrlite and olivine clinopyroxenite corresponds to diopside in the chemical composition, whereas that in gabbro–amphibolite compositionally corresponds to augite. In the massif, pyroxene shows an increase in the iron mole fraction and a decrease in the Ca content upward. The content of ilmenite increases from early high-Mg to late low-Mg magmatic rocks; the mineral composition also changes: the Mn concentration increases, whereas the Mg content shows opposite behavior.

ANALYTICAL TECHNIQUES

The results of an analytical study of rocks and ores at the Institute of Geochemistry, Siberian Branch, Russian Academy of Sciences, Irkutsk are used. The petrogenic elements were examined by bulk chemical analysis and X-ray fluorescence. Cr, Ni, Cu, Co, and Zn ore elements were measured by atomic absorption spectroscopy using an S4 Pioneer instrument equipped with a Rh anode and operating at a voltage of 40 kV and current intensity of 50 mA.

The PGE concentration in rocks of the Kingash and Idar complexes was determined by an improved method of Au and PGE determination at a level of 1–10 ng/g using inductively coupled plasma mass spectrometry (ICP-MS) (Vlasova et al., 2007).

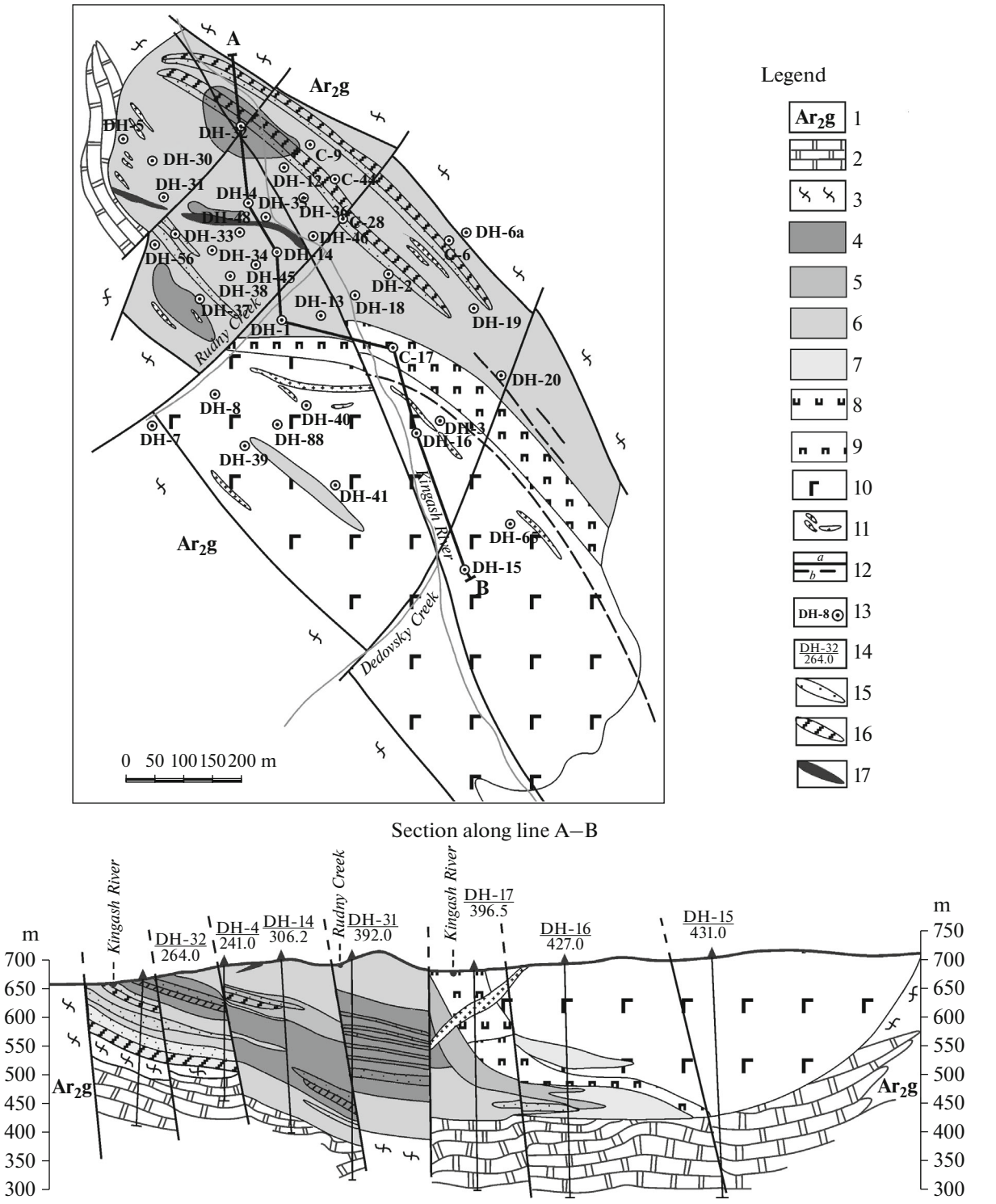

Fig. 2. Geological sketch map of Kingash massif (on materials of Kingash geological exploration crew, Institute of Geochemistry, Siberian Branch, Russian Academy of Sciences, and Geokomp LLC (Lomaeva and Tarasov, 2010)). (1) Upper Archean Karagan structural complex, gneiss sequence with interacations (AR_2g) of (2) marble and (3) crystalline schist; (4–10) rocks of Kingash massif: (4) dunite, (5) wehrlite, (6) dunitic serpentinite, (7) wehrlitic serpentinite, (8) olivine clinopyroxenite, (9) clinopyroxenite, (10) metaggabro; (11) Upper Archean Tuksha migmatite–plagiogranite complex ($\gamma AR_2?tk$); (12) faults: (a) identified, (b) probable; (13) and their position; (14) borehole position in section, borehole number in numerator and depth in denominator; (15–16) Ni–Cu–PGE ores: (5) raw (0.5–1 wt % Ni), (16) high-grade (>1 wt % Ni); (17) breccias–vein ore.

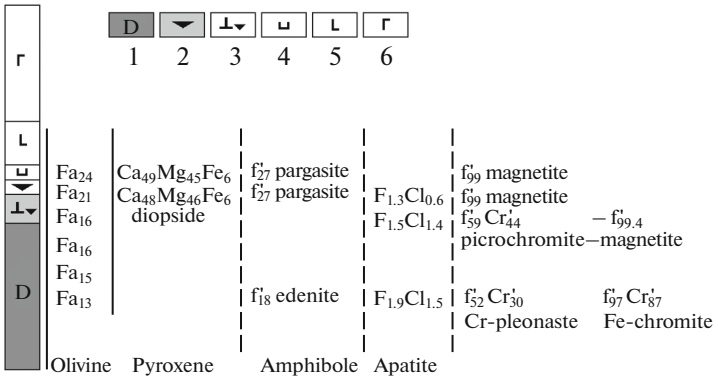

Fig. 3. Variation in chemical composition of minerals along section of massif. Solid and dash lines depict intervals for mineral precipitating as cumulus and intercumulus phase, respectively. (1) dunite, (2) wehrlite, (3) wehrlitic serpentinite, (4) olivine clinopyroxenite, (5) clinopyroxenite, (6) gabbro-amphibolite.

PGM were found and their chemical composition was measured using a JXA-8200 JEOL electron microprobe equipped with a high-resolution electron microscope, an EDS with SiLi detector with 133 eV resolution, and five WD spectrometers.

PGM were found as fine inclusions in sulfide minerals using a scanning electron microscope and identified by EDS. The chemical composition of inclusions was determined by WD spectrometry. The conditions for excitation and detection of the analytical signal were as follows: accelerating voltage 20 kV, current intensity 20 nA, and beam diameter 1 μm. Concentrations were calculated by the ZAF method. Pure metals Pt, Pd, Ru, Re, Bi, and Te; alloys Fe, Ni, Co, and Ag–Au; and pyrrhotite (Fe, S) were used as standards.

MINERAL ASSEMBLAGES OF SULFIDES AND THEIR DISTRIBUTION IN THE MASSIF ROCKS

Sulfides are disseminated in all rocks of the Kingash massif, but the chalcopyrite–pentlandite–pyrrhotite assemblage typical of ultramafic rocks is of industrial interest. In the Ni content, which is the major industrial constituent, the ores are divided into high-grade (>1 wt %), raw (0.5–1 wt %), and low-grade (0.2–0.5 wt %) (Lomaeva and Tarasov, 2010). Nearly all ultramafic rocks of the massif are orebodies, because their Ni content is rarely below the cutoff grade of 0.2 wt %. Barren wehrlite and replacing serpentinite at the contact with amphibolite, as well as thin rock layers within the ultramafic part of the massif, are an exception. Alternating low-grade, raw, and high-grade ores with Ni concentrated at the bottom of the massif distinguish the petrographic zoning in the section.

The ores of the Kingash deposit are characterized by variable proportions of pyrrhorite, pentlandite, and chalcopyrite group minerals (Table 1), which reflects the different physicochemical conditions of ore deposition. Several ore types are identified by their structure and texture: disseminated, densely disseminated, breccia–vein, and massive. Pyrrhotite or pentlandite is usual the predominant sulfide in them; chalcopyrite is less frequent. Disseminated pyrrhotite with subordinate chalcopyrite and pentlandite is predominant in gabbro and pyroxenite.

The thickness of separated horizons of the chalcopyrite–pyrrhotite–pentlandite ore type exceed 150 m with a length up to 700 m. Valleriite, the most refractory copper-bearing mineral, is characteristic of disseminated pyrrhotite–pentlandite ore in serpentinized rocks.

A horizon of densely disseminated ore 10 m thick was uncovered at a depth of 150–200 m; it contains mackinawite in addition to pentlandite–pyrrhotite mineralization. Breccia–vein ore (5 m in thickness) was found at the surface in the central part of the ore field and uncovered by some boreholes at depth. Massive pentlandite–cubanite–chalcopyrite–pyrrhotite ore containing up to 5.7 and 1.8 wt % Cu and Ni, respectively, and 500 ppm Co were found at the bottom of the massif. The maximum sulfur content reaches 15.91 wt % in massive ore and 5.7 wt % in olivine clinopyroxenite. Pyrrhotite rather than pentandite is the major ore mineral of disseminated ore in olivine pyroxenite; therefore, the Ni content in it does not exceed 1300 ppm.

A horizon of disseminated chalcopyrite–pyrrhotite–pentlandite ore 5–10 m thick with a high grade of Ni (0.81–1.49 wt %), Cu (0.22–0.82 wt %), Au (0.58–0.84 ppm), and PGE up to 17 ppm, called the PGE horizon no. 1 or reef (Glazunov et al., 2003), was uncovered by boreholes in wehrlitic serpentinite in the northern part of the massif. Its specific features are abnormal enrichment in Pt and Pd as compared to hanging wall rocks and a sulfide content not higher than 8 vol % (Glazunov and Radomskaya, 2010) (Fig. 4).

Pyrrhotite, pentlandite, and chalcopyrite are the major ore minerals at the Kingash deposit. Sulfide dis-

Table 1. Description of ores in ultramafic rocks of Kingash massif

Ore type	Disseminated	Densely disseminated	Breccia–vein	Massive
Mineralogical variety	Chalcopyrite–pentlandite–pyrrhotite, chalcopyrite–pyrrhotite, pentlandite–pyrrhotite, pentlandite		Chalcopyrite–cubanite–pentlandite–pyrrhotite	
Content of ore minerals, vol %	0.1–16	22–50	50–95	70–95
Content of minerals, vol %				
Sulfides				
Pyrrhotite	0.6–4	11–38	25–28	44–50
Pentlandite	0.6–6	2.6–4	11–20	18
Chalcopyrite	0.3–2.7	0.8–1.8	3–20	21–25
Cubanite	few grains–0.8	0.5–2	0.4–5	1–5
Secondary minerals				
Valleriite	0.8–1.5	0.1–2	0.1	1–3
Mackinawite	0.5–1	0.5–1.2	0.7–5.5	e.з.
Oxides				
Magnetite	2–13	5.5	0.1–3.5	2.5–3.5
Chromite	0.2–3	0.1	0.1	0.1
Ilmenite	s.g.–1	s.g.–1.5	0.5–2	2.5–4.5
Gangue constituents	Olivine, clinopyroxene (diopside), amphibole, serpentine, chlorite, mica (phlogopite), apatite		Serpentine, amphibole, chlorite, mica (phlogopite), apatite	
Structure	Disseminated, schlieren–veinlet–disseminated, banded		Spotted	Massive
Texture	Fine-grained, sideronitic, pod-disseminated, exsolved (lattice, lamellar)			
Shape of orebodies	Sheetlike, lenticular		Lenticular, vein	
Size of orebody	Up to 250 m	5–10 m	From 1–10 cm to до 3–5 m	
Ni grade, wt %	0.2 cut-off grade; 0.2–0.5 low-grade ore; 0.5–1.0 raw ore; >1.0 high-grade ore		>1.0 high-grade ore	

semination composed of troilite, hexagonal pyrrhotite, and Fe-rich pentlandite is characteristic of dunite and wehrlite. Breccia–vein and massive ores are composed of hexagonal and monoclinic pyrrhotite, nickeloan pentlandite, and chalcopyrite. Hexagonal pyrrhotite with flamelike lamellae of troilite, pentlandite, and chalcopyrite are common in wehrlite serpentinite of the platinum horizon, and in breccia–vein and massive ores. The Fe content in pyrrhotite decreases from early to late differentiates (Fig. 5). The Fe content (at %) in pyrrhotite from dunite, wehrlite, and massive ore ranges from 49.1 to 52.3, from 48.2 to 51.1, and from 46.5 to 49.5, respectively. The lowest Fe content was determined in pyrrhotite from amphibolized gabbro (46.5–47.9 at %). The Fe/S value decreases from 1.91 to 1.52, whereas the Ni content increases from trace amounts to 0.4 wt % in pyrrhotite from early disseminated to breccia–vein and massive ore; the Fe/S value decreases from 1.00 to 0.85 in chalcopyrite; the Fe/Ni value decreases from 1.93 to 1.03 in pentlandite. Chalcopyrite and cubanite are the most abundant minerals of the Cu–Fe–S system at the Kingash deposit; talnakhite, bornite, and chalcocite are less frequent.

The change in the composition of ore minerals, namely, decreasing Fe content and increasing S, Ni, and Co concentrations from early magmatic low-grade disseminated ore to late magmatic breccias–vein and massive ores, indicate the evolution of sulfide melt during its crystallization.

MINERALOGY OF PLATINUM GROUP METALS

The following PGM and Ag–Au compounds have been established at the Kingash deposit: michenerite, merenskyite, kotulskite, sobolevskite, froodite, paolovite, cabriite, stibiopalladinite, Pd-melonite, sperrylite, moncheite, tetraferroplatinum, platarsite, irarsite, iridarsenite, erlichmanite, and hessite, as well as

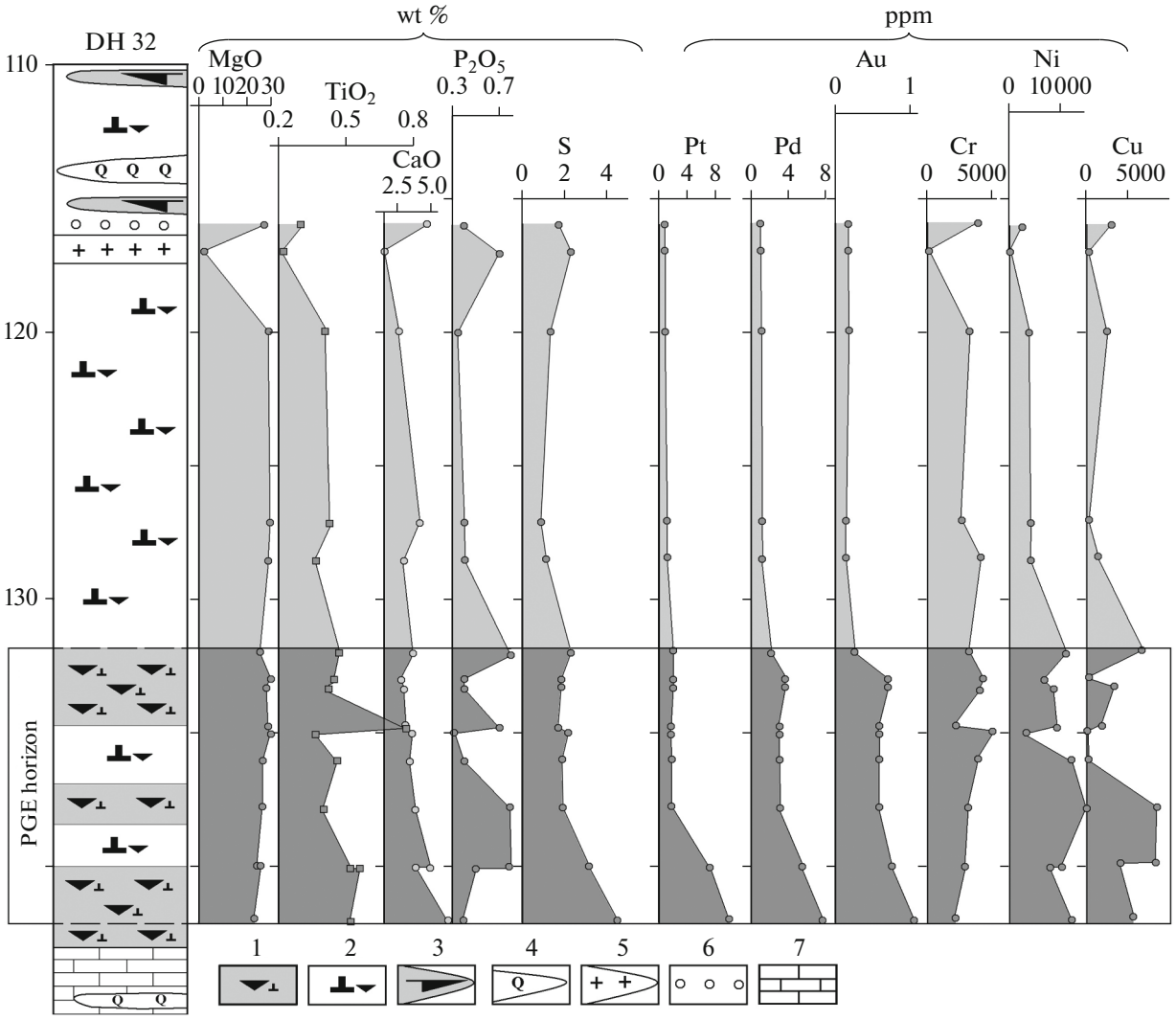

Fig. 4. Variation in content of rock-forming oxides and ore elements along section. (1) serpentinized wehrlite, (2) wehrlitic serpentinite, (3) gabbro-amphibolite, (4) quartz veins, (5) plagiogranite, (6) talc rock, (7) marble.

native, Cu- and Pd-bearing gold, electrum, küstelite, auricupride, Pd tetraauricupride, and Au–Ag amalgam. Compounds of the Pd–Bi–Te system (Fig. 6), which are predominant over other PGM, are the most abundant in ultramafic rocks of the massif. Similar PGM assemblages are also typical of other massifs within the Sayan zone (Mekhonoshin et al., 2013). Pd bismuthotellurides at the Kingash deposit are distinguished by a high Bi/Te value and low Pt content with elevated Sb and Ni concentrations (Tables 2, 3).

Table 4 lists the most abundant PGM assemblages in disseminated ores. Michenerite is found in both disseminated and breccia–vein ores. Michenerite + merenskyite + hessite ± kotulskite ± altaite and michenerite + sperrylite assemblages found in sulfide aggregates of pyrrhotite and pentlandite and chalcopyrite and amphibole, respectively, are characteristic of disseminated ore. In breccia–vein ore, tiny crystals of michenerite (1–5 × 5–10 μm) occur in pyrrhotite veinlets and are intergrown with altaite, froodite, and hessite.

Concentrations of the major and trace elements in michenerite of the Kingash massif are variable with the following pattern: the Bi content decreases, whereas the Pd and Te contents increase from disseminated to breccia–vein ore (Table 3). An elevated Fe content (0.36–0.45 wt %) in the mineral was recorded (see Table 2).

Merenskyite predominates in disseminated ore, but it has not been found in the breccia–vein type. Merenskyite + michenerite + hessite and merenskyite + cobaltite assemblages (Figs. 8a, 8b) were identified within the PGE horizon. The sulfide aggregates containing clusters of bismuthotellurides and hessite are high-Ni pentlandite and hexagonal pyrrhotite with flamelike lamellae of trolilite (Fig. 8b). Merenskyite of

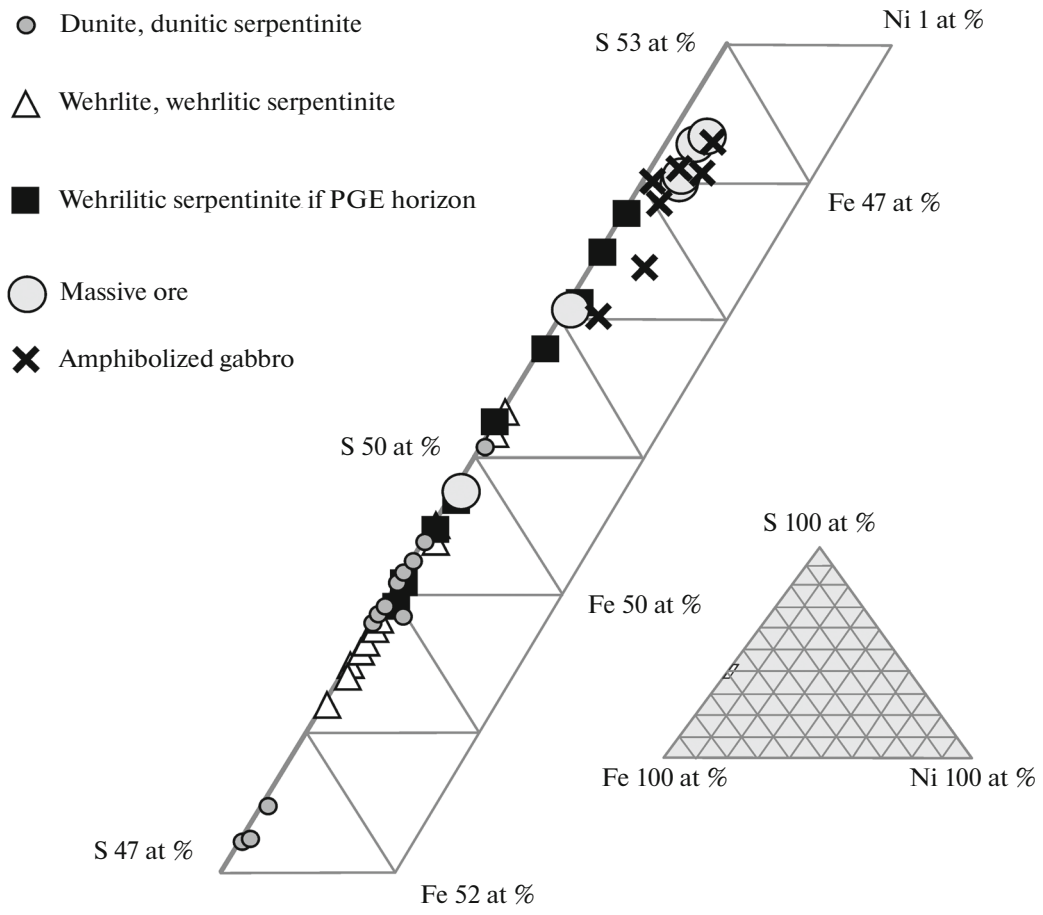

Fig. 5. Triangular plot in terms of Fe–S–Ni (at %) illustrating composition of pyrrhotite and troilite from ultramafic and mafic rocks of Kingash massif. Our unpublished data and data taken from (Glazunov et al., 2003) and (Kozyrev at al.,1999) are used.

the Kingash massif forms a solid solution series with Pd-melonite and is characterized by highly variable contents of major components Pd, Bi, Te, and Ni (Fig. 7), showing clear increasing Ni and Te contents and decreasing Pd concentration from dunite to wehrlite (Fig. 9, Table 3). Pd-melonite was predominantly found in disseminated ore of wehrlitic serpentinite (see Table 2).

Kotulskite is associated with michenerite, merenskyite, hessite, and altaite in disseminated ore and with sobolevskite in breccia–vein ore. Kotulskite from disseminated ore in wehrlite contains substantial Pt and Ag, 1.4 and 1.6 wt %, respectively. Sobolevskite contains Os (0.3 wt %) and Ir (0.27 wt %). The Sb concentration in sobolevskite decreases from 3.5–7.7 to 0.23–0.61 wt % as transited from disseminated to breccia–vein ore. Froodite found in wehrlitic serpentinite is associated with irarsite, altaite, ± michenerite, and hessite. It contains admixtures (wt %): 0.2–0.9 Os, 0.3–3.9 Ir, and 2.5–3.5 As.

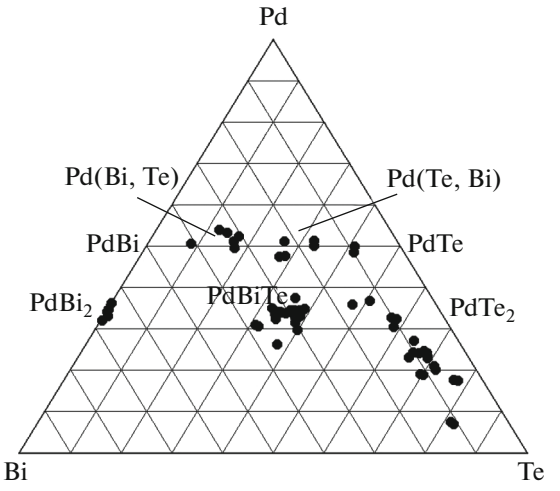

Fig. 6. Triangular plot illustrating compositions of Pd–Bi–Te system minerals in Kingash massif. Data taken from Table 3, and (Glazunov et al., 2003) and (Shvedov et al., 1997, 2001) are used here and in Fig. 7.

Table 2. Chemical composition (wt %) of Pd–Bi–Te system minerals from wehrlite serpentinite of Kingash deposit

Number	Pd	Bi	Te	Pt	Fe	Ag	Ni	Total	Formula
Michenerite									
1	22.60	40.32	31.83	0.21	–	4.37	0.48	100.42	$(Pd_{0.96}Ag_{0.18}Ni_{0.04})_{1.18}Te_{1.13}Bi_{0.87}$
2	24.27	43.33	30.28	<0.1	0.36	0.93	0.23	99.59	$(Pd_{1.03}Ag_{0.04}Ni_{0.02})_{1.08}Te_{1.07}Bi_{0.93}$
3	23.94	42.26	33.06	<0.1	0.40	<0.09	0.24	100.03	$(Pd_{0.98}Ni_{0.02})_{1.00}Te_{1.12}Bi_{0.88}$
4	22.26	41.56	33.07	0.38	0.40	2.48	0.15	100.38	$(Pd_{0.91}Ag_{0.10}Ni_{0.01})_{1.03}Te_{1.13}Bi_{0.87}$
5	22.91	41.64	33.67	0.2	0.45	0.80	0.17	99.83	$(Pd_{0.93}Ag_{0.03}Ni_{0.01})_{0.97}Te_{1.14}Bi_{0.86}$
Merenskyite									
6	18.40	11.52	63.27	<0.1	0.17	<0.09	6.19	99.84	$(Pd_{0.63}Ni_{0.38})_{1.02}Te_{1.80}Bi_{0.20}$
7	18.32	11.31	64.52	<0.1	0.15	0.10	6.28	100.82	$(Pd_{0.62}Ni_{0.38})_{1.00}Te_{1.81}Bi_{0.19}$
8	18.07	12.11	63.45	<0.1	0.33	<0.09	6.33	100.32	$(Pd_{0.61}Ni_{0.39})_{1.00}Te_{1.79}Bi_{0.21}$
9	18.01	11.63	63.29	0.2	0.31	<0.09	6.47	99.99	$(Pd_{0.61}Ni_{0.40})_{1.02}Te_{1.80}Bi_{0.20}$
Pd-melonite									
11	9.67	15.17	62.34	0.19	1.19	2.91	7.77	99.29	$(Ni_{0.47}Pd_{0.32}Ag_{0.10}Fe_{0.08})_{0.97}Te_{1.74}Bi_{0.26}$

(1) DH-4-97.15 breccia–vein, (2–11) S-32-139 disseminated ore of PGE horizon. Total of composition 1 includes, wt %: 0.55 Ru, 0.27 Rh, 0.3 Re. Dash demotes element content is below detection limit. PGM compositions were measured on a JXA-8200 electron microprobe, analyst L.F. Suvorova.

Sperrylite, predominant Pt-bearing mineral associated with michenerite, was found in chalcopyrite and silicate matrix at various ore horizons of the deposit including rocks in the surface mines. Sperrylite contains admixture of refractory Ir and Os. This feature was recorded in sperrylite from the Ognit and Tartai massifs in Alkhadyr Terrane (Biryusa block) (Mekhonoshin et al., 2013) and was determined as typical feature of platiniferous massifs in the East Siberian metallogenic province (Polyakov et al., 2013). The Ir admixture is characteristic of sperrylite from dunite (0.4–2.2 wt %), whereas in sperrylite from wehrlite and rocks in the oxidation zone, it decreases to trace amounts (Glazunov et al., 2003).

Glazunov et al. (2003) described the only finding of moncheite $(Pt_{0.86}Pd_{0.04}Ag_{0.03})_{0.94}(Te_{1.65}Bi_{0.35})_2$ in the high-grade ore. Among Pd–Sb compounds, stibiopalladinite occurred as grains up to 0.5 mm intergrown with amphibole and gold in disseminated ore, and mertieite associated with electrum and auricupride from supergene zone were described (Glazunov et al., 2003). Occasional grains of paolovite are enclosed in pyrrhotite of breccia–vein ore. Admixtures of Ir and Os up to 0.14 wt % were measured in the mineral.

The Re mineral with grain size of 0.5 × 4.5 μm (Fig. 8d) was found in pyrrhotite veinlet for the first time within the Kingash massif. It was identified with EDS. Rhenium minerals are described from patiniferous ores of the Stillwater massif (Tarkian et al., 1991).

Hessite the major Ag carrier at the deposit is associated with michenerite, merenskyite, sobolevskite, and kotulskite. The assemblage of Au, Ag, and Cu compounds and mertieite II is found in the supergene zone. Here, separated grains of sperrylite are found. An absence of other PGM is due to the stability of sperrylite in the supergene zone as demonstrated for ores of the Chiney massif (Tolstykh et al., 2008). The high Pd content 2–4 and 1.7 wt% was measured in tetraauricupride and copper- and palladium-bearing gold, respectively.

Thus, the michenerite + merenskyite + hessite ± kotulskite ± altaite ± Pd-melonite assemblage is typical of early magmatic disseminated ore, whereas separated grains of michenerite and paolovite, and the sobolevskite + kotulskite and altaite + froodite ± irarsite ± hessite ±michenerite are formed in breccia-vein ore at the late magmatic stage. Most PGM were found in sulfides, whereas the higher-temperature sperrylite and sobolevskite + altaite assemblage were found in amphibole and chlorite, respectively.

GEOCHEMISTRY OF PLATINUM GROUP ELEMENTS

In the rocks of the Kingash massif, the MgO content decreases with increasing SiO_2, CaO, Al_2O_3, TiO_2, Na_2O, and K_2O contents (Table 5) reflecting magmatic fractionation. Sulfide-bearing rocks of the Kingash massif are ores with the economic PGE grade, among which Pd and Pt are the most abundant. According to the study of drill core from ultramafic section, the PGE, Ni, and Cu contents tend to increase with depth. However, the content of PGE in rocks does not always correlate with that of Ni and Cu (see Fig. 4). The PGE content increases from dunite to wehrlite and decreases in gabbro and clinopyroxenite. Pt is predominant over Pd in dunite and wehrlitic ser-

Table 3. Chemical composition (wt %) of platinum group minerals from ores of Kingash deposit

Ore type and number of analyses	Pd	Bi	Te	Pt	Sb	As	Sn	Fe	Ni
Michenerite									
Disseminated	22.6–24.9	40.1–45.9	28.6–31.9	<0.1	0.1–0.2			0.1–0.4	0.2–0.5
10	24	42.5	30.4	<0.1	0.1			0.3	0.2
Vein–breccia	24.4–29.6	25.7–45.3	28.6–47.8		<0.03–0.9				
10	26.1	39	35.6		0.2				
Merenskyite									
Disseminated	13.9–30.1	13.2–20.1	50.1–63.5	<0.1–0.2				<0.1–0.3	0.8–8.6
13	23.4	16.2	57.3	0.1				0.2	3.2
Ore of PGE horizon	11.7–18.4	6.3–14.0	54.4–65.1	<0.1–0.4				0.2–2.5	5.0–9.6
14	16.0	10.6	61.9	0.1				1.1	6.9
Kotulskite									
Disseminated	36.9–41.8	14.5–38.4	25.3–41.0		<0.03–4.09				
8	39.9	25.9	33.4		1.1				
Vein–breccia	36.7–36.8	25.3–25.5			0.3				
2	36.8	25.4			0.3				
Sobolevskite									
Disseminated	36.8–38.5	44.4–46.0	10.2–15.1	<0.1	1.3–7.7	<0.01			
7	37.7	45.3	11.9	<0.1	5	<0.01			
Vein–breccia	36.1–38.3	46.9–47.5	14.8–15.5	<0.1	0.2–0.6	<0.01			
6	37.6	47.2	15.2	<0.1	0.4	<0.01			
Froodite									
Vein–breccia	18.5–21.2	70.8–78.8	<0.1–0.53			3.5			
6	19.9	75.5	0.2						
Mertieite									
Disseminated	71.2–72.0				26.5–28.6	1.7–3.1			
5	71.5				27.0	2.8			
Stibiopalladinite									
Disseminated	63.6–67.5		<0.1	<0.1–0.8	24.0–29.8	0.6–3.1			
3	65.8		<0.1	0.4	26.6	2.2			
Pd-melonite									
Disseminated	4.6–14.4	14.0–16.5	63.5–65.0						8.6–15.0
3	8.0	14.9	64.6						12.8
Paolovite									
Vein–breccia	64.0–64.7	<0.03	<0.03				36.2–36.7		
3	64.4	<0.03	<0.03				36.4		
Sperrylite									
Disseminated				53.0–56.0		42.3–44.2			
8				54.6		43.2			
Maucherite									
Disseminated	0.4–0.5			0.6		50.3		0.1–0.3	48.8–50.0
3	0.4			0.6		50.3		0.2	49.4

Table 4. Assemblages of PGM and other minerals in disseminated ore of Kingash massif

Mineral with PGM inclusions	Assemblage
In dunite serpentinite	
Amphibole	Merenskyite + kotulskite + altaite + michenerite + hessite ± Rh-gersdorffite
Chlorite	Sperrylite
Pyrrhotite	Merenskyite + michenerite + hessite
Pentlandite	Sobolevskite + gersdorffite + nickeline
Pentlandite	Michenerite + Pd-melonite + Co-gersdorffite + hessite ± coloradoite
Pentlandite	Gersdorffite + molybdenite
Pentlandite	Merenskyite + michenerite ± Sb-kotulskite ± hessite ± gersdorffite
Pentlandite	Michenerite + altaite + hessite
Pentlandite	Tetraferroplatinum + nickeline
Chalcopyrite	Merenskyite + michenerite + Hg-hessite + Co-gersdorffite
Chalcopyrite	Sperrylite + michenerite
Chalcopyrite	Merenskyite + michenerite + hessite + kotulskite + altaite
Chalcopyrite	Michenerite + hessite + Co-gersdorffite
In wehrlitic serpentinite	
Pyrrhotite	Merenskyite + michenerite + hessite + kotulskite + cobaltite
Pyrrhotite	Irarsite + froodite + altaite

pentinite of the PGE horizon, whereas in wehrlite the reverse is true (Table 5).

A direct correlation between the Pt, Pd, and Au contents and Ni and S contents is observed for the disseminated sulfide ore containing 0.45–1.1 ppm Pd and 0.45–0.8 ppm Pt (Fig. 10). The increase in Pd content from early disseminated to late ores is consistent with the experimental data on Pd fractionation in residual melt (Distler et al., 1977, 1988; Sinyakova 1998; Kolonin and Sinyakova, 2005). The PGE distribution within the PGE horizon with the highest PGE grade (0.7–9.8 ppm Pt, 1.5–7.6 ppm Pd) differs from that in raw disseminated ore. Rocks of the PGE horizon with high Pt, Pd, and Au and low S are in separate fields in the binary plots. This PGE distribution character is due to a fluid constituent contributing to PGE migration (Boudreau et al., 1986). This is supported by abundant minerals containing such volatiles as edenite, pargasite, biotite, and chlor- and fluorapatite in the PGE horizon. It is noteworthy that the highest-grade PGE ores of the PGE horizon are the richest in REE (Radomskaya and Glazunov, 2009). The REE distribution patterns of high-grade disseminated ore containing Ni > 1.0 wt % are shown in black in Fig. 11. The low REE content (4–5 ppm) in densely disseminated high-grade ore in dunite indicates that this rock formed at the early magmatic stage as a result of sulfide gravity separation. High-grade ore with high REE (20–25 ppm) and elevated TiO_2, Zr, Y, and Nb contents in wehrlitic serpentinite of the PGE horizon crystallized at the late magmatic stage from a more highly fractionated residual melt saturated in Cl, F, and H_2O contributing to the PGE transportation. Breccia–vein ore from wehrlitic serpentinite in which Re minerals were found is the richest in this element (66 ppb).

Low-melting PGE (Pt, Pd, Rh) dominate refractory PGE (Os, Ir, Ru) (Fig. 12a). The PGE distribution trends in ultramafic rocks of the Kingash massif differ from those in arc and oceanic island basalts (Fig. 12b). The Os, Pd, and Au concentrations in rocks with high PGE content are higher than in the Merensky Reef of the Bushveld Complex (Fig. 12b). Like other massifs within the Sayan zone, an elevated concentration of refractory elements in the Kingash massif is typical of the dunite–peridotite–pyroxenite–gabbro assemblage and is caused by the higher degree of melting of the mantle substrate during the formation of the parental magma of these massifs (Polyakov et al., 2013; Mekhonoshin et al., 2013).

Comparison of ultramafic rocks with the identical MgO content from the mineralized Kingash and barren Idar complexes (Table 5) shows that the latter differs by low Al_2O_3 and TiO_2 and elevated SiO_2. The ultramafic rocks of the Idar Complex correspond in Ni content to low-grade and off-grade ores of the Kingash massif, but it is nearly Cu-free or its grade is below the detection limit (<20 ppm), whereas in Kingash rocks, the Cu grade is highly variable (ppm): from 80 to 6200 in dunite and from 30 to 8200 in wehrlite. The PGE content in ultramafic rocks of the Idar Complex is comparable to that in low-grade and off-grade ores of the Kingash Complex. These specific features made it possible to determine the criteria of ore content in ultramafic rocks within the Kan block.

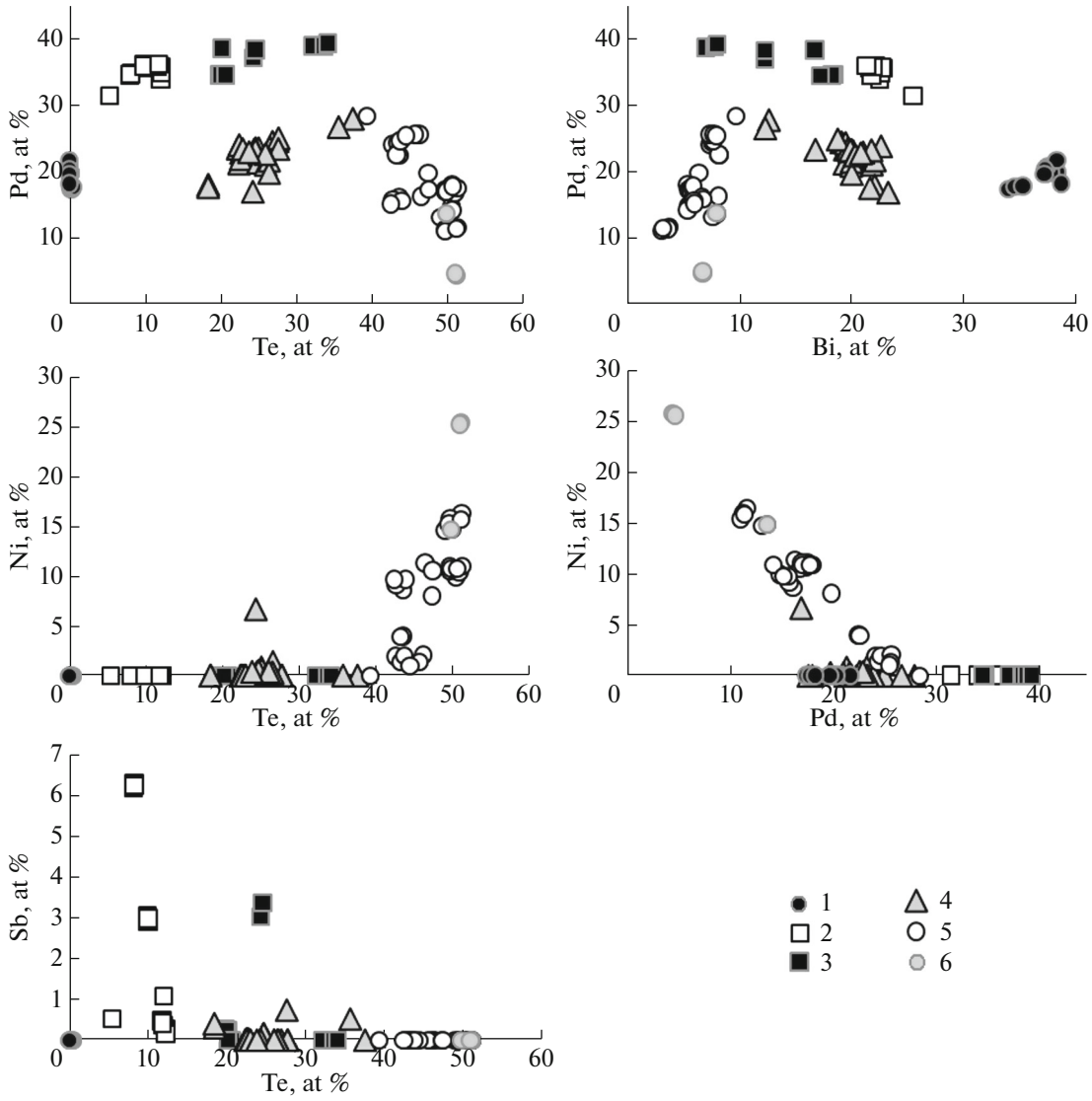

Fig. 7. Binary plots illustrating composition of Pd–Bi–Te system minerals in Kingash massif. (1) Froodite, (2) sobolevskite, (3) kotulskite, (4) michenerite, (5) merenskyite, (6) Pd-melonite.

Low Ni/Cu (2.8–10.5) and Cr/Ti (0.8–4.5), and high Pd/Rh (23–180) and Pt/Rh (11.1–547.5) values with highly variable Ni content are typical of Kingash ultramafic rocks as compared to those in ultramafic rocks of the Idar Complex: 105 Ni/Cu, 105, 6.0 Cr/Ti, 6.4 Pd/Rh, and 4.8 Pt/Rh.

DISCUSSION

Currently, there are several genetic models for the Kingash massif.

(1) The model of differentiated intrusion of the basalt–picrite assemblage with multichamber feeders providing input of additional rich melt responsible for ore deposition. The source of parental silicate melt with the ore constituent was at a depth corresponding to spinel facies (T ~ 1000°C, P ~10–15 kb) (*Platinonosnost'* ..., 1995). Glazunov et al. (2003) drew attention to the genetic relation of ultramafic rocks and only part of gabbroic rocks, which is spatially related to peridotite and graduates to the later.

(2) Kornev and Ekhanin (1997) suggested that the Kingash massif is a member of the Kingash basalt–komatiite volcanic complex. However, the komatiite hypothesis has been refuted by the different spectra of precious metals in ultramafic rocks of the Kingash massif and komatiite (Fig. 12a) and the absence of spinifex texture in Kingash rocks. The latter is an important feature of komatiite, proving that the high-Mg rocks belong to komatiite and indicating rapid melt solidification under submarine or air conditions.

(3) Chernyshov et al. (2004) considered the massif as a subvolcanic intermediate chamber, whereas the deep-seated fault at the center of the massif is a feeder

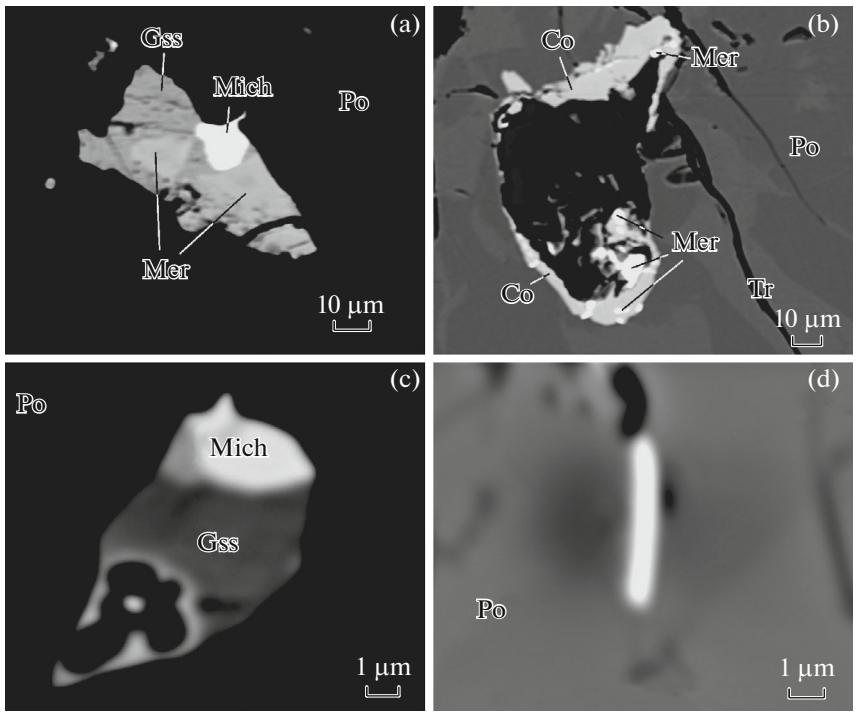

Fig. 8. Backscattered electron images of PGM from rocks of Kingash massif. (a, b, c) PGM of PGE horizon: (a) hessite (Gss) with merenskyite (Mer) and michenerite (Mich), (b) rim of cobaltite (Co) and merenskyite enclosed in pyrrhotite (Po) with lamellae of troilite (Tr), (c) hessite with michenerite enclosed in pyrrhotite; (d) Re mineral enclosed in pyrrhotite from vein–breccia ore. Images were obtained on a Jeol JXA-8200 electron microprobe.

for picrite–komatiite melt emplaced into the upper part of the Earth's crust and effused on the surface. Gabbroic rocks are the second intrusion phase postdating ultramafic rocks.

(4) Glotov et al. (2004) considered the Kingash massif as a subvolcanic intrusion that rapidly solidified in a near-surface environment.

(5) Gertner et al. (2005, 2009) validated the formation of the massif during three stages: ultramafic rocks and associated gabbro-amphibolite at 1410 Ma (Sm–Nd), a gabbroic body and pyroxenite zone at 875 Ma

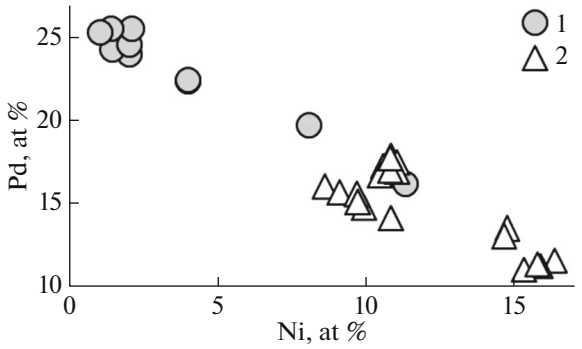

Fig. 9. Pd versus Ni plot for merenskyite of Kingash deposit. (1) Dunite and dunitic serpentinite, (2) wehrlitic serpentinite.

(Sm–Nd), and the final metamorphic stage at 495 Ma (Rb–Sr). Monomineralic fractions (Gertner's data) and whole rocks (Glazunov's data) were studied.

The U–Pb age of baddeleyite from ultramafic rocks is 726 Ma (Ernst et al., 2012), which is much younger and synchronous with the formation of the Taratai massif in the Biryusa block, 712 ± 6 Ma and the Yoko-Dovyren massif in Transbaikalia, 728 ± 6 Ma (Ariskin et al., 2013).

The problem of the spatiotemporal relationship between ultramafic rocks and gabbro, as well as pyroxenite formation, never became irrelevant. For example, some researchers agree that the rocks in the contact zones of such massifs are formed as a result magmatic alteration of ultramafic rocks by a mafic melt (Zavaritsky, 1961; Lesnov, 1986).

The above review of genetic models shows that there no agreement stems from detailed studies about the origin of the Kingash massif. Petrochemical and geochemical data indicate that the rocks of the massif resulted from magmatic differentiation of parental picritic magma (Radomskaya and Glazunov, 2009; Radomskaya, 2012). The high $^{87}Sr/^{86}Sr$ and low εNd values of Kingash rocks (Glazunov et al., 2003) correspond to the EM-II mantle component and plot in the field of oceanic islands in the $^{143}Nd/^{144}Nd$ versus $^{87}Sr/^{86}Sr$ diagram (Faure, 1986) (Fig. 13).

Table 5. Chemical composition of rocks of Kingash and Idar Complexes

Number of sample	DH-1-110	DH-1-116	DH-4-77	DH-4-95.5	DH-4-164	DH-31-42	DH-32-140
Number of analysis	1	2	3	4	5	6	7
SiO_2, wt %	37.47	36.25	38.82	35.38	38.73	37.45	36.17
TiO_2	0.17	0.14	0.17	0.47	0.35	0.6	0.52
Al_2O_3	2.42	2.17	2.4	3.2	4.1	6.9	6.9
Fe_2O_3	4.49	4.1	5.03	3.05	7.72	5.32	5.49
FeO	7.45	7.54	7.9	12.93	4.31	8.09	8.87
MnO	0.18	0.16	0.17	0.14	0.15	0.15	0.13
MgO	40.5	39.24	37.5	28.2	30.6	25.24	24.3
CaO	0.73	0.73	1.4	3.0	2.6	4.96	5.0
Na_2O	<0.20	<0.26	0.85	0.77	0.74	0.48	0.35
K_2O	0.27	0.02	0.08	0.61	0.11	0.09	0.07
P_2O_5	–	0.02	0.03	0.06	0.06	0.08	0.08
S_{tot}	0.2	1.2	0.39	2.19	0.69	1.8	2.84
LOI	4.58	5.83	3.48	8.66	8.08	5.76	6.83
Total ΣI	99.02	98.17	99.47	100.23	99.37	98.6	99.28
Sr, ppm	<20	<20	–	–	–	65	86
Cr	2500	2500	6400	3100	4900	3400	2900
Ni	1500	3200	4200	9900	4600	9300	10300
Co	120	150	160	310	200	240	215
Cu	65	1100	1000	2400	4600	3300	8200
V	39	44	79	72	260	186	161
Zr	15	10	17	49	30	31	32
Sc	8	<2	19	<2	<2	22	19
Os, ppb	<0.1	<0.1	<0.1	60.4	0.72	11.8	7.1
Ir	0.68	1.21	6.6	14	10.2	8.37	22.9
Ru	1.31	2.7	7.5	126.6	5.4	20.1	95.7
Rh	0.9	1.27	7.65	29	4.8	10	9.2
Pt	32.6	86.8	244.9	322	2628	236	1942
Pd	21.8	29.2	191.9	700.9	277	554	1656
Re	0.7	6	3.9	66.6	6.7	14.7	19.6
Pd/Pt	0.7	0.3	0.8	2.2	0.1	2.3	0.9
Pt/Rh	36.2	68.3	32.0	11.1	547.5	23.6	211.1
Pd/Rh	24.2	23.0	25.1	24.2	57.7	55.4	180.0
Ni/Cu	23.1	2.9	4.2	4.1	1.0	2.8	1.3
Cr/Ti	2.1	2.6	4.5	1.0	1.9	0.8	0.8

Table 5. (Contd.)

Number of sample	DH-17-146	DH-17-155.5	DH-3-172	06-IG-4A	DH-20-348	06-IG-34A	06-IG-33
Number of analysis	8	9	10	11	12	13	14
SiO_2, wt %	45.53	46.52	44.79	39.54	45.59	53.25	52.55
TiO_2	0.34	0.4	0.42	0.05	1.154	0.34	2.177
Al_2O_3	3.33	3.14	10.18	0.6	13.71	15.45	12.35
Fe_2O_3	12.26	13.05	13.57	3.95	12.19	2.91	17.75
FeO				3.31		5.09	
MnO	0.11	0.13	0.03	0.13	0.169	0.14	0.196
MgO	20.19	21.5	12.48	31.28	9.902	7.83	3.065
CaO	14.63	11.93	15.01	6.5	13.61	10.65	6.838
Na_2O	0.35	0.36	0.67	<0.01	1.67	1.01	2.57
K_2O	0.1	0.13	0.36	<0.01	0.593	0.59	2.205
P_2O_5	0.04	0.04	0.02	0.03	0.115	0.04	0.265
S tot	–	–	–	0.13	–	–	–
LOI	3.08	2.75	2.62	13.18	1.31	2.27	0.19
Total ΣI	100.62	100.68	100.4	99.28	100.2	99.62	100.16
Sr, ppm	<30	<30	170	38	996	16	95
Cr	3700	3400	1000	2100	660	255	–
Ni	980	1800	850	2200	380	130	–
Co	200	220	140	71	48	44	–
Cu	780	600	390	21	86	36	–
V	350	360	250	25	30	190	–
Zr	50	33	<30	0.6	161	–	248
Sc	60	74	60	7	30	–	–
Os, ppb	<0.1	0.86	<0.1	<0.1	<0.1	<0.1	<0.1
Ir	1.68	1.45	1.88	1.71	4.32	5.9	8.7
Ru	0.23	0.4	0.43	5.1	2.4	0.16	1.4
Rh	0.62	1.49	<0.1	5	<0.1	<0.1	<0.1
Pt	10.8	12.7	18.9	23.9	24.7	15.7	23.4
Pd	5.6	10.6	24.2	31.9	10.4	5.9	8.8
Re	9.2	6.8	6.2	0.65	0.8	0.22	0.06
Pd/Pt	0.5	0.8	1.3	1.3	0.4	0.4	0.4
Pt/Rh	17.4	8.5	189.0	4.8	247.0	157.0	234.0
Pd/Rh	9.0	7.1	242.0	6.4	104.0	59.0	88.0
Ni/Cu	1.3	3.0	2.2	104.8	4.4	3.6	–
Cr/Ti	1.6	1.2	0.3	6.0	0.1	0.1	–

(1–10) Rocks of Kingash massif: (1) dunite, (2–3) mineralized dunite, (4–6) mineralized wehrlite serpentinite, (7) wehrlite serpentinite of PGE horizon, (8–9) clinopyroxenite, (10) metagabbro, (11, 13, 14) country amphibolite, (12) serpentinite of Idar Complex. Total in compositions (1–13) include Cr_2O_3 and NiO, wt %: 0.37 and 0.19 (1), 0.37 and 0.41 (2), 0.76 and 0.49 (3), 0.45 and 1.12 (4), 0.66 and 0.47 (5), 0.5 and 1.18 (6), 0.42 and 1.31 (7), 0.54 and 0.12 (8), 0.50 and 0.23 (9), 0.15 and 0.11 (10), 0.30 and 0.28 (11), 0.10 and 0.05 (12), and 0.04 and 0.02 (13). Dash denoted element content is velow detection limit. Compositions were determined at Institute of Geochemistry, Siberian Branch, Russian Academy of Sciences: silicate analysis (analyst T.V. Ozhogina), X-ray fluorescent analysis (analysts T.N. Gunicheva, A.K. Klimova, A.L. Finkelstein), and quantitative spectral analysis (analyst S.S. Vorobiova). PGE content was measured with ICP-MS using improved procedure (Vlasova et al., 2007) at level of 1 to 10 ng/g (analysts V.N. Vlasova, V.I. Lozhkin, V.I. Menshikov).

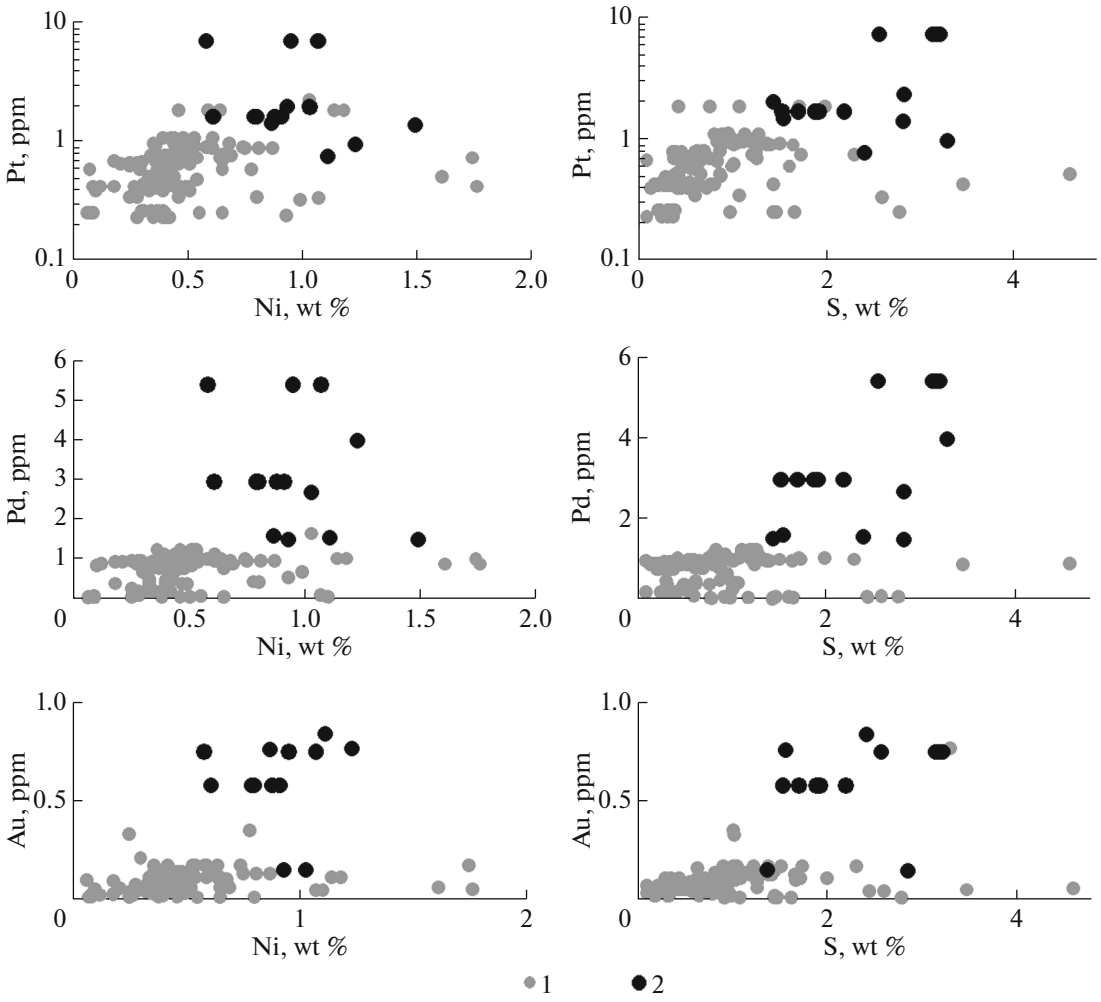

Fig. 10. Binary plots illustrating relationships between Pd, Pt, and Au contents and S and Ni concentrations in rocks and ores of Kingash massif. (1) Disseminated and densely disseminated ores, (2) wehrlitic serpentinite of PGE horizon.

The problem of the source for sulfur and metals forming ore in rocks is fundamental for sulfide formation. According to Naldrett (2003), the average Ni content is 1750 ppm for a MgO content of 32 wt % in ultramafic magma from which sulfide minerals precipitated. The Ni content in ultramafic rocks of the Kingash massif is almost double, 3140 ppm for a MgO content of 31 wt % (Glazunov, 2003). This raises questions about the reasons for the elevated content of metals in the melt from which Ni–Cu–PGE ores crystallized. As is known, silicate magmas are considered a metal source for sulfides, whereas sulfides are formed as a result of melt saturation of sulfur. The sulfur solubility in melts of various compositions for various P–T parameters was experimentally studied many times and was estimated as 0.071 to 2.09 wt % (Connoly and Haughton, 1972; Kuznetsova and Krigman, 1978; Almukhamedov et al., 1974; Shima and Naldrett, 1975; Gorbachev and Nrekrasov, 1979; Mysen and Popp, 1980; Kostyuk, 2011). The sulfur solubility in an ultramafic melt has been established as very low, ranging from 0.008 to 0.92 wt % (Almukhamedov and Medvedev., 1982; Connoly and Haughton, 1972; Shima and Naldrett,1975; Kostyuk, 2011). The inconsistency in the low solubility of sulfur in melt according to experimental data and its high content in natural objects has resulted in several hypotheses of sulfur concentration in melts in the area of magmatic formation of sulfides at large deposits: liquation of magma (Godlevsky, 1968), infiltration-autometasomatic (Zolotokhin, 2001), sulfurization owing to assimilation of S-bearing country rocks (Almukhamedov and Medvedev, 1982), transmagmatic fluid affecting magmatic differentiates (Marakushev et al., 2014), and "sulfur interception" (Malyshev, 2004).

The PGE content in ultramafic–mafic massifs is conventionally associated with deep-seated magmatism. In this case, platinum and palladium mineralization is associated with chromite and nickel–copper sulfide ore, respectively. According to the experimen-

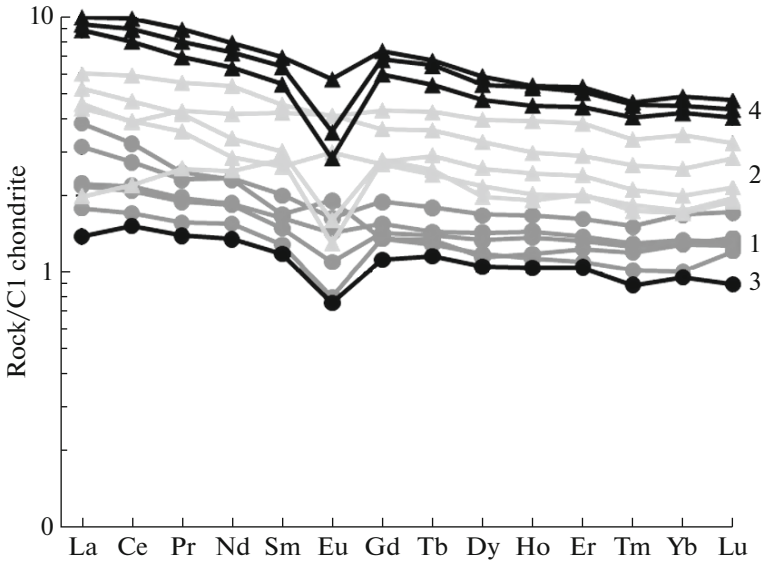

Fig. 11. C1 chondrite (Boynton, 1984) normalized REE distribution patterns for rocks of Kingash massif, modified after (Radomskaya and Glazunov, 2009). (1) Dunite and dunitic serpentinite; (2) wehrlite and wehrlitic serpentinite; (3, 4) high-grade ore with Ni content higher than 1.0 wt %: (3) dunitic serpentinite, (4) wehrlitic serpentinite of PGE horizon.

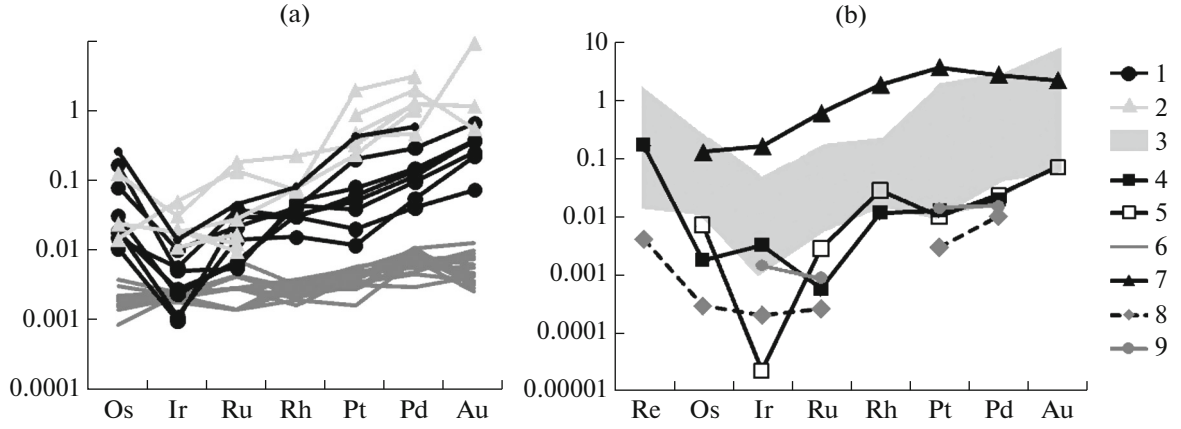

Fig. 12. C1 chondrite (McDonough and Sun, 1995) normalized precious metal distribution patterns. (a) Ultramafic rocks of Kingash massif: (1) dunite and dunitic serpentinite, (2) wehrlite and wehrlitic serpentinite; (b) rocks of Kingash massif: (3) ultramafic rocks, (4) pyroxenite, (5) metagabbro; (6) komatiite of Barberton Mountain Land (Maier et al., 2003); (7) Merensky Reef (Hiemstra, 1979); (8) Island Arc Basalt (OIB) (McDonough and Sun, 1995; Woodland et al., 2002); (9) Oceanic Island Basalt (OIB) (Chazey and Neal, 2005).

tal data, sulfide–silicate separation in the sulfide–silicate system is accompanied by layering of sulfide melt to form two sulfide liquids: high-S Fe–Ni and low-S Cu–Fe enriched in Pt (Ebel and Naldrett, 1996; Gorbachev et al., 1993; Marakushev et al., 2014). However, the discovery of sulfide-poor PGE reefs has resulted in a new hypothesis of pneumatolytic genesis of PGM (Ryabov et al., 1999, 2000; Boudreau et al., 1986).

Picrite melt is a source for Cu, Ni, and PGE in the ores of the Kingash deposit. The δS^{34} value ranging from –1.4 to +2.0 ‰ in Kingash ores (Glotov et al., 2004) is close to that of mantle sulfur ranging from 0 to 3.0‰. The formation temperature and pressure of kingash ultramafic rocks (T ~ 1260–1060°C, P ~ 15–13 kb) are characteristic of an abyssal environment (Radomskaya, 2012). Chrome spinel, olivine, clinopyroxene, and high-Mg hornblende crystallize from ultramafic melt at magmatic stage. The content of ilmenite increases from dunite to wehrlite with decreasing Mg and increasing Mn contents in this mineral (Radomskaya, 2012). Sulfide melt is separated from ore silicate melt as silicate minerals crystallize to form a monosulfide solid solution (Mss), from which

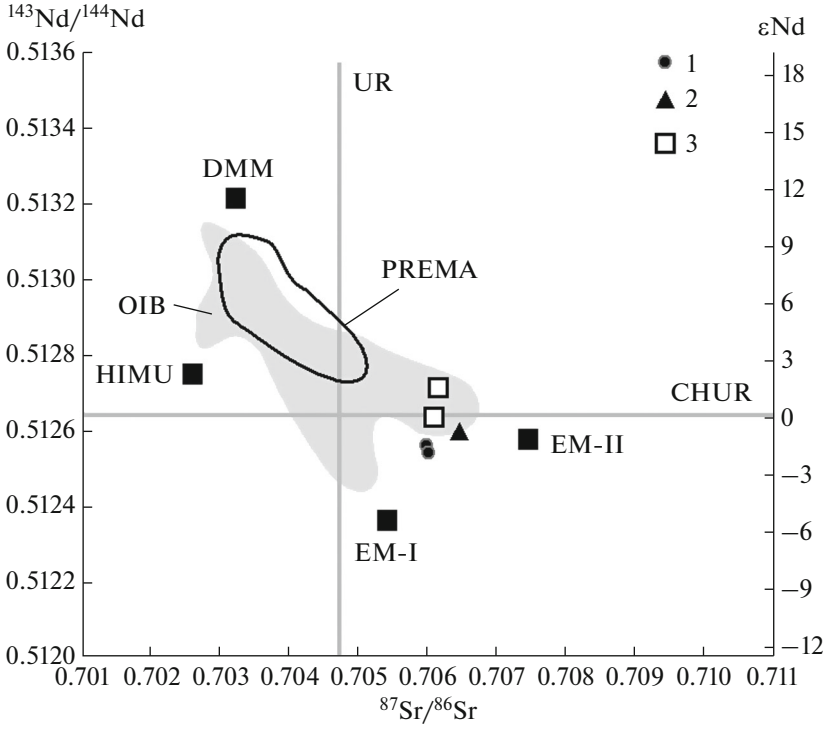

Fig. 13. Position of rocks of Kingash massif in system of global mantle components in $^{143}Nd/^{144}Nd$ versus $^{87}Sr/^{86}Sr$ diagram (Faure, 1986). (1) Dunite, (2) serpentinized wehrlite, (3) gabbro–amphibolite. (UR) Uniform Reservoir, (CHUR) CHondrite Uniform Reservoir, (PREMA) PREvalent Mantle, (DMM) Depleted Mantle MORB (Middle Oceanic Ridge Basalt), (EM-I, EM-II) Enriched Mantle I and II, (OIB) Ocean Island Basalt.

pyrrhotite and pentlandite are formed (Kolonin et al., 2005; Karup-Møller et al., 1995; Kullerud et al., 1969). This separation starts at the early magmatic stage during forsterite crystallization, which is supported by spheroidal sulfide inclusions found in this mineral (Glazunov and Radomskaya, 2010). Liquation origin of very large and high-grade sulfide Ni–Cu deposits of Norilsk, Talnakh, and Pechenga, which are important producers of copper, nickel, cobalt, and PGE, was suggested by Godlewski in 1968. As demonstrated by experiments in sulfide systems, sulfide liquids are always layered to matte and Mss; this process is called fractionation crystallization (Ebel and Naldrett, 1996).

During solidification of sulfide melt, sulfide liquid fills interstices between previously formed crystals of silicate minerals to form the early magmatic disseminated ore with predominant minerals of the Fe–Ni–S system, whereas immiscible residual sulfide melt accumulates chalcophylic elements derived from coexisting silicate melt as a result of which ore is enriched in the minerals of the Cu–Fe–S system. The concentration of sulfide droplets at the bottom of the massif due to gravity results in the formation of densely disseminated ore. Among the first refractory elements, Os and Ir precipitate from the melt in chrome spinel and sperrylite; Pd tellurides and biusmuthides are later. Breccia–vein pentlandite–chalcopyrite–cubanite–pyrrhotite ore is formed as a result of sulfide liquid input into reduced zones. At this stage, michenerite and hessite crystallize from sulfide melt and proper Re phases start to crystallize.

The formation of horizons with high PGE and Ni contents within the Kingash massif requires genetic explanation. Currently, there are magmatic and hydrothermal–metasomatic models for the origin of PGE reefs. The first is that silicates, sulfides, and PGE are the magma crystallization products and PGE are accumulated in a reef as a result of (a) in situ differentiation, (b) decantation, and (c) emplacement of new magma into the magma chamber (Naldrett et al., 1982; Campbell et al., 1983; Kruger and Marsh, 1985). According to the second model, fluids contained in magma lead to redistribution of PGE ascending through the crystallized melt (Elliott et al., 1982; Boudreau et al. et al., 1986).

The PGE horizons of the Kingash massif are late melt differentiates, which is supported by the high PGE content in them. Abundant H_2O-bearing minerals, such as hornblende and apatite in these horizons, indicate the presence of fluid components (Cl, F, P) in the residual fluid, which contributed to the transportation of PGM, according to experimental data (Boudreau et al., 1986). Intergrowth of apatite and sulfides indicates simultaneous crystallization of these miner-

als. Low-melting and volatile compounds accumulated in the melt as it cooled. These compounds reacted with the earlier high-temperature compounds. Disseminated ore in dunite and wehrlite is a product of fractionation crystallization, whereas densely disseminated ore resulted from concentration of sulfide melt under the influence of gravity.

CONCLUSIONS

The compositional evolution of sulfide minerals from early high-Mg to late low-Mg rocks, sulfide droplets associated with accessory chrome spinel in olivine, and sulfide–apatite intergrowths in late differentiates with high REE indicate that sulfide melt separated from ore silicate melt during the entire formation period of rocks of the massif as rock-forming minerals crystallized.

In the Kingash massif, PGE are predominantly contained in chalcopyrite–pyrhotite–pentlandite ore and make up Pd bismuthotellurides. Mineral assemblages in Ni–Cu–PGE ores of the Kingash massif evolved with decreasing Mg# in the rocks: michenerite + merenskyite + hessite ± kotulskite ± altaite and michenerite + sperrylite in ore dunite; michenerite + froodite ± hessite without sperrylite in mineralized wehrlite; merenskyite + michenerite + hessite and merenskyite + cobaltite the ore of the PGE horizon; separate grains of michenerite and paolovite, and sobolevskite + kotulskite and alatite + froodite ± irarsite ± hessite ± michenerite assemblages in breccia–vein ore.

The melt from which the Kingash rocks formed evolved during differentiation. This is manifested in the Pd/Pt value increasing from 0.1 to 4.2 with Mg# decreasing (down to 1.9 and 4.2 in dunite and wehrlite, respectively). During evolution of the Kingash ore system, PGM were progressively enriched in Ni (from 0.8 to 9.6 wt % Ni in merenskyite) similarly to sulfide minerals, and the Ni, Cu, Co, PGE and Re contents increased from early disseminated to late vein–breccia ore.

The PGE and contents S positively correlate in disseminated ore and show a negligible correlation in the PGE horizon richer in PGE and REE. Therefore, high-grade ore of the massif formed at the early and late magmatic stages. In the first case, it was the product of liquid immiscibility and gravitational separation (densely disseminated pentlandite–pyrrhotite ore with subordinate Fe-rich chalcopyrite). In the second case, it formed from the residual melt saturated in volatiles contributing to the transportation and segregation of PGE (disseminated chalcopyrite–pentlandite–pyrrhotite ore with PGM of the PGE horizon).

From the comparison of the ore and PGE contents in ultramafic rocks of the mineralized Kingash and barren Idar Complexes, the criteria of ore content in ultramafic rocks of the Kansk block were identified. Geochemical indicators of the ore-bearing Kingash-type ultramafic rocks in the Kansk block are: high contents of alkalis, TiO_2 (>0.1 wt %), Cu (>35 ppm), low Ni/Cu (2.8–10.5) and Cr/Ti (0.8–4.5) values, and high Pd/Rh (23–180) and Pt/Rh (11.1–547.5) values.

ACKNOWLEDGMENTS

We are grateful to analysts of the Institute of Geochemistry, Siberian Branch, Russian Academy of Sciences T.V. Ozhogina, Yu.V. Sokolnikova, I.Yu. Voronova, G.Ya. Strezhneva, E.V. Smirnova, T.N. Gunicheva, A.L. Finkelstein, S.S. Vorobiova, and V.I. Lozhkin. We thank A.A. Vorontsov and N.V. Vladykin for their valuable advice in discussing the results of the study.

REFERENCES

Al'mukhamedov, A.I. and Medvedev, A.Ya., *Geokhimiya sery v protsessakh evolyutsii osnovnykh magm (Sulfur Geochemistry in the Evolution of Basic Magmas)*, Moscow: Nauka, 1982.

Al'mukhamedov, A.I., Medvedev, A.Ya., Solomonova, L.A., and Taroev, V.K., Sulfur solubility in basic silicate melts and some geochemical sequences, *Geokhimiya,* 1974, no. 11, pp. 1672–1681.

Altukhov, E.N., Gershanik, S.Yu., Glazunov, O.M., and Mekhonoshin, A.S., Tectonic setting and ore potential of the basite–ultrabasite rocks of the Northern Baikal region, *Geol. Geofiz.,* 1990, no. 6, pp. 56–64.

Ariskin A.A., Kostitsyn, Yu.A., Danyushevsky, L.V., Meffre, S., Nikolaev, G.S., McNeill, E., Kislov E.V., and Orsoev, D.A., Geochronology of the Dovyren intrusive complex, northwestern Baikal Area, Russia, in the Neoproterozoic, *Geochem. Int.,* 2013, vol. 51, no. 11, pp. 859–875.

Boudreau, A.E., Mathez, E.A., and McCallum, I.S., Halogen geochemistry of the Stillwater and Bushveld complexes: evidence for transport of the platinum-group elements by Cl-rich fluids, *J. Petrol.,* 1986, vol. 27, no. 4, pp. 967–986.

Boynton, W.V., *Cosmochemistry of the rare earth elements. meteorite studies, Rare Earth Element Geochemistry. Development in Geochemistry,* Amsterdam: Elsevier, 1984, vol. 2, pp. 63–114.

Campbell, I.H., Naldrett, A.J., and Barnes, S.J., A model for the origin of the platinum-rich sulfide horizons in the Bushveld and Stillwater complexes, *J. Petrol.,* 1983, vol. 24, pp. 133–165.

Chazey, III, W.J. and Neal, C.R., Platinum-group element constraints on source composition and magma evolution of the Kerguelen plateau using basalt from ODP leg 183, *Geochim. Cosmochim. Acta,* 2005, vol. 69, no. 19, pp. 4685–4701.

Chernyshov, A.I., Nozhkin, A.D., Stupakov, S.I., et al., Kingash mafite–ultramafite massif: geological setting, inner structure, composition, and petrostructural analysis of ultramafites, East Sayan, *Platina Rossii. Sb. nauch. Trudov* (Platinum of Russia. A Collection of Papers), Moscow: *Geoinformmark*, 2004, vol. 5, pp. 152–175.

Connoly, J.W.D. and Haughton, D., R. The valence of sulfur in glass of basaltic composition formed under conditions of low oxidation potential, *Am. Mineral.,* 1972, vol. 57, nos. 9–10, pp. 1515–1517.

Distler, V.V., Grokhovskaya, T.L., Evstigneeva, T.L., et al., *Petrologiya sul'fidnogo magmaticheskogo rudoobrazovaniya (Petrology of Sulfide Magmatic Ore Formation)*, Moscow: Nauka, 1988.

Distler, V.V., Malevskii, A.Yu., and Laputina, I.P., PGE distribution between pyrrhotite and pentlandite during crystallization of sulfide melt, *Geokhimiya,* 1977, no. 11, pp. 1646–1658.

Dobretsov, N.L., Borisenko, A.S., Izokh, A.E., and Zhmodik, S.M., A thermochemical model of Eurasian Permo-Triassic mantle plumes as a basis for prediction and exploration for Cu–Ni–PGE and rare-metal ore deposits, *Russ. Geol. Geohys.,* 2010, vol. 51, no 9, pp. 903–924.

Ebel, D.S. and Naldrett, A.J., Fractional crystallization of sulfide ore liquids at high temperature, *Econ. Geol.,* 1996, vol. 91, pp. 607–621.

Elliott, W.C., Grandstaff, D.E., Ulmer, G.C., et al., An intrinsic oxygen fugacity study of platinum-carbon associations in layered intrusions, *Econ. Geol.,* 1982, vol. 77, pp. 1493–1510.

Ernst, R.E., Hamilton, M.A., and Soderlund, U., A proposed 725 Ma Dovyren–Kingash lip of southern Siberia, and possible reconstruction link with the 725–715 Ma Franklin lip of northern Laurentia, *Abstract volume 35, Geological Association of Canada (GAC)–Mineralogical Association of Canada (MAC) Joint Annual Meeting, Geoscience at the Edge,* St. John's, Newfoundland and Labrador, 2012, vol. 35, pp. 27–29.

Faure, G., *Principles of Isotope Geochemistry,* New York: Wiley, 1986.

Gertner, I.F., Glazunov, O.M., Morikyo, T., Tishin, P.A., Chernyshov, A.I., Krasnova, T.S., and Vrublevsky, V.V., Isotope-geochemical constraints on the genetic model of the Kingash ultramafic–mafic massif, East Sayan, *Petrologiya magmaticheskikh i metamorficheskikh kompleksov. Vyp. 5. Mater. Vseross. Petrograf. Konf.* (Petrology of Magmatic and Metamorphic Complexes, Iss. 5. All-Russia Petrographic Conference), Tomsk: *TsNTI*, 2005, vol. 1, pp. 61–72.

Gertner, I.F., Vrublevsky, V.V., Glazunov, O.M., Tishin, P.A., Krasnova, T.S., and Voitenko, D.N., Age and source material of the Kingash ultramafic–mafic massif, East Sayan, *Dokl. Earth Sci.,* 2009, vol. 429, pp. 1526–1532.

Glazunov, O.M., Prospective nickel–platinum province of South Siberia, *Problemy geologii Sibiri* (Geological Problems of Siberia), Tomsk: *TGU*, 1994, vol. 2, p. 83.

Glazunov, O.M., Prospects of expansion of the mineral–raw base of non-ferrous metals in the Sayan nickel–platinum province, *Tsvetnye metally Sibiri. 2009. Sb. dokl. pervogo mezhdunar. kongr. v sostave XV Mezhdunar. konferentsii-vystavki "Alyuminii Sibiri" III Konferentsii "Metallurgiya tsvetnykh i redkikh metallov" V simp. "Zoloto Sibiri". Razdel 1. Mineral'no-syr'evaya baza tsvetnykh metallov* (Non-ferrous Metals of Siberia. 2009. Reports of the First International Congress on the 15th International Conference–Exhibition "Aluminum of Siberia", 3rd Conference "Metallurgy of Non-Ferrous and Trace Metrals", 5th Symposium "Gold of Siberia". Section 1. Mineral–Raw Base of Non-Ferrous Metals), Krasnoyarsk: Verso, 2009, pp. 19–24.

Glazunov, O.M., Bognibov, V.I., and Ekhanin, A.G., *Kingashskoe platinoidno-medno-nikelevoe mestorozhdenie (Kingash Platinum–Copper–Nickel Deposit)*, Irkutsk: IGTU, 2003.

Glazunov, O.M. and Radomskaya, T.A., Geochemical model of genesis of the Kingash platinoid–copper–nickel deposit, *Dokl. Earth Sci.,* 2010, vol. 430, pp. 71–75.

Glotov, A.I., Krivenko, A.P., and Lavrenchuk, A.V., PGM geochemistry and physicochemical features of the formation of the Kingash sulfide platinum–copper–nickel deposit, East Sayan, *Platina Rossii. Sb. nauch. trudov.* (Platinum of Russia, A Collection of Papers), Moscow: *Geoinformmark*, 2004, vol. 5, pp. 195–204.

Godlevskii, M.N., Magmatic deposits, *Genezis endogennykh rudnykh mestorozhdenii* (Genesis of Endogenous Ore Deposits), Moscow, 1968, pp. 7–83.

Goldschmidt, V.M., *Geochemistry,* Oxford: Clarendon Press, 1954.

Gorbachev, N.A. and Nekrasov, I.Ya., Sulfur content in silicate melts of the $FeS–FeO–SiO_2–K_2O–H_2O–CO_2$ system at pressure of 1, 5, and 10 kbar, *Problemy petrogenezisa i rudoobrazovaniya. Korrelyatsiya endogennykh protsessov. Tez. dokl.* (Problems of Petrogenesis and Ore Formation Correlation of Endogenous Processes), Irkutsk, 1979, p. 25.

Gorbachev, N.S., Brugmann, G., Naldrett, A., et al., Redox conditions and distribution of platinum metals in the sulfide–silicate magmatic systems, *Dokl. Akad. Nauk,* 1993, vol. 331, no. 2, pp. 220–223.

Hiemstra, S.A., The role of collectors in the formation of platinum deposits in the Bushveld complex, *Can. Mineral.,* 1979, vol. 17, pp. 469–482.

Izokh, A.E., Vishnevskii, A.V., Polyakov, G.V., Shelepaev, R.A., Age of picrite and picrodolerite magmatism in western Mongolia, *Russ. Geol. Geophys.,* 2011, vol. 52, no. 1, pp. 7–23.

Karup-Moller, S. and Makovicky, E., The phase system Fe–Ni–S at 725°C, *Neues. Jahrb. Mineral. Monatsh,* 1995, no. 1, pp. 1–10.

Kolonin, G.R. and Sinyakova, E.F., High-temperature sulfide solid solutions as intermediate reservoirs for PGE accumulation in natural and technological processes, *Platina Rossii. Sb. nauch. Trudov* (Platinum of Russia. A Collection of Papers), Moscow: *Geoinformmark*, 2005, vol. 6, pp. 180–188.

Kornev, T.Ya., Ekhanin, A.G., Knyazev, V.N., and Sharifulin, S.K., *Zelenokamennye poyasa yugo-zapadnogo obramleniya Sibirskoi platformy i ikh metallogeniya* (Greenstone Belts of the Framing of the Siberian Platform and their Metallogeny), Krasnoyarsk: KNIIGiMS, 2004.

Kostyuk, A.V. Experimental Modeling of Liquid Immiscibility in the Sulfide–Silicate–Carbonate Mantle Magmas, *Extended Abstract of Candidate (Geol-Min.) Dissertation,* Moscow, 2011.

Kozyrev, S.M., Simonova, V.F., Dedeev, A.V., Valetov, A.V., Lyul'ko, V.A., and Rezniko, I.G., New technology of reworking of disseminated sulfide platinum–copper–nickel ores of the Kingash deposit, *Platina Rossii. Sb. nauch. trudov.* (Platinum of Russia. A Collection of Papers), Moscow: *Geoinformmark*, 1999, vol. 4, pp. 214–227.

Kruger, F. J. and Marsh, J. S., The mineralogy, petrology and origin of the Merensky cyclic unit in the western Bushveld Complex, *Econ. Geol.,* 1985, vol. 80, pp. 958–974.

Kullerud, G., Yund, R.A., and Moh, G.H., *Phase relations in the Cu–Fe–S, Cu–Ni–S, and Fe–Ni–S-systems, Econ. Geol. Monograph,* Wilson, H.D.B., Ed., 1969, vol. 4.

Kuzmin, M.I. and Yarmolyuk, V.V., Mantle plumes of Centra Asia and their role in the formation of endogenous deposits, *Russ. Geol. Geophys.,* 2014, vol. 55, no. 2, pp. 120–143.

Kuznetsova, S.Ya. and Krigman, L.D., Sulfur solubility in silicate melts–-models of natural magmas, *Geokhimiya,* 1978, no. 2, pp. 238–247.

Lesnov, F.P. *Petrokhimiya poligennykh bazit-giperbazitovykh plutonov skladchatykh oblastei (Petrochemistry of Polygenetic Mafic–Ultramafic Plutons of Fold Areas)*, Novosibirsk: Nauka, 1986.

Lomaeva, G.R. and Tarasov, A.V., Kingash deposit of sulfide noble metal–copper–nickel ores: first in East Sayn, *Razved. Okhr. Nedr,* 2010, no. 9, pp. 28–31.

Maier, W.D., Roelofse, F., and Barnes, S.-J., The concentration of the platinum-group elements in South African komatiites: implication for mantle sources, melting regime and PGE fractionation during crystallization, *J. Petrol.,* 2003, vol. 44, no. 10, pp. 1787–1804.

Malyshev, A.I., *Sera v magmaticheskom rudoobrazovanii (Sulfur in the Magmatic Ore Formation)*, Yekaterinburg: IGG UrO RAN, 2004.

Marakushev, A.A., Paneyakh, N.A., and Marakushev, S.A., *Sul'fidnoe rudoobrazovanie i ego uglevodorodnaya spetsializatsiya* (Sulfide Ore Formation and its Hydrocarbon Specialization), Moscow: GEOS, 2014. 184 s.

McDonough, W.F. and Sun, S.-S., The composition of the Earth, *Chem. Geol.,* 1995, vol. 120, pp. 223–253.

Mekhonoshin, A. S., Tolstykh, N. D., Podlipskii, M. Yu., Kolotilina, T. B., Vishnevskii, A. V., and Benedyuk, Yu. P., PGE mineralization of dunite–wehrlite massifs at the Gutara–Uda interfluve, Eastern Sayan, *Geol. Ore Deposits,* 2013, vol. 55, no. 3, pp. 162–175.

Mysen, B.O. and Popp, R.K., Solubility of sulfur in $CaMgSi_2O_6$ and $NaAlSi_3O_8$ melt at high pressure and temperature with controlled fO_2 and fS_2, *Am. J. Sci.,* 1980, vol. 280, no. 1, pp. 78–92.

Naldrett, A.J., *Magmaticheskie sul'fidnye mestorozhdeniya medno-nikelevykh i platinometal'nykh rud* (Magmatic Sulfide Deposits of Copper–Nickel and Platinum Ores), St. Petersburg: SPbGU, 2003.

Naldrett, A.J., Innes, D.G., Sowa, J., and Gorton, M.P., Compositional variations within and between five Sudbury ore deposits, *Econ. Geol.,* 1982, vol. 77, no. 6, pp. 1519–1534.

Nozhkin, A.D. and Smagin, A.N., A new scheme of the subdivision of the Precambrian metamorphic complexes of the Kan block, East Sayan, *Geol. Geofiz.,* 1988, no. 12, pp. 3–12.

Nozhkin, A.D., Turkina, O.M., Bibikova, E.V., and Ponomarchuk, V.A., Structure, composition and formation conditions of metasedimentary-volcanogenic complexes of the Kan greenstone belt, northwestern Sayan region), *Russ. Geol. Geophys.,* 2001, vol. 42, no. 7, pp. 1058–1078.

Nozhkin, A.D., Chernyshov, A.I., Turkina, O.M., et al., Metasedimentary-volcanogenic and intrusive complexes of the Idar greenstone belt (East Sayan), *Petrologiya magmaticheskikh i metamorficheskikh kompleksov* (Petrology of Magmatic and Metamorphic Complexes), Tomsk: *TsNTI*, 2005, vol. 2, pp. 356–384.

Platinonosnost' ul'trabazit-bazitovykh kompleksov Yuga Sibiri (Platinum Potential of the Ultramafic–Mafic Complexes of South Siberia), Bognibov, V. I., Krivenko, A.P., Izokh, A. E., et al., Novosibirsk: SO RAN NITS OIGGM, 1995.

Polyakov, G.V., Tolstykh, N.D., Mekhonoshin, A.S., Izokh, A.E., Podlipskii, M.Yu., Orsoev, D.A., and Kolotilina, T.B., Ultramafic–mafic igneous complexes of the Precambrian east Siberian metallogenic province (southern framing of the Siberian Craton), *Russ. Geol. Geophys.,* 2013, vol. 54, no. 11, pp. 1689–1704.

Radomskaya, T.A., Mineralogy and Geochemistry of the Kingash Platinum–Copper–Nickel Deposit, East Sayan, *Extended Abstract of Candidate (Geol-Min.) Dissertation,* Irkutsk: Inst. Geograf. im. V.B. Sochavy SO RAN, 2012.

Radomskaya, T.A. and Glazunov, O.M., Rare-metal composition of rocks and ores of the Kingash-type platinum–copper–nickel deposits, *Geologiya, poiski i razvedka rudnykh mestorozhdenii* (Geology and Prospecting of Ore Deposits) Irkutsk: IrGTU, 2009, pp. 37–42.

Ryabov, V.V., Fluid regime of the trap magmatgism and ore formation (petrological aspect), *Geol. Geofiz.,* 1999, vol 40, no. 10, pp. 1457–1473.

Ryabov, V.V., Shevko, A.Ya., and Gora, M.P., *Magmaticheskie obrazovaniya Noril'skogo raiona. Petrologiya trappov (Magmatic Rocks of the Norilsk District. Petrology of Traps)*, Novosibirsk: Nonparel', 2000, vol. 1.

Sez'ko, A.I., *Main stages in the formation of continental crust of the Sayan region, Evolyutsiya zemnoi kory v dokembrii i paleozoe. Sayano-Baikal'skaya gornaya oblast (Crustal Evolution in the Precambrian and Paleozoic)*, Novosibirsk: Nauka, 1988, pp. 7–40.

Shima, H. and Naldrett, A.J., Solubility of sulfur in an ultramafic melt and relevance of system Fe–S–O, *Econ. Geol.,* 1975, vol. 70, no. 5, pp. 960–967.

Shvedov, G.I., Nekos, V.V., Tret'yakov, N.A., New data on mineralogy of the mafic–ultramafic massifs of the Kingash ore district (East Sayan), *Platina v geologicheskikh formatsiyakh Sibiri. Programma "Platina Rossii"* (Platinum in Geological Formations of Siberia. Program "Platinum of Russia"), Krasnoyarsk: KNIIGiMS, 2001, pp. 134–137.

Shvedov, G.I., Tolstykh, N.D., Nekos, V.V., and Pospelova, L.N., PGE minerals in the sulfide copper–nickel ores of the Kingash Massif (East Sayan), *Geol. Geofiz.,* 1997, vol. 38, no. 11, pp. 1842–1848.

Sinyakova, E.F., Forms of palladium segregations during crystallization of sulfide melts of the Fe–Ni–S system at sulfur content from 40 to 51 at %, *Geol. Geofiz.,* 1998, vol. 39, no. 5, pp. 627–639.

Tarkian, M., Hously, R.M., Volborth, A., Greis, O., and Moh, G.H., Unnamed Re–Mo–Cu sulfide from the Stillwater Complex, and crystal chemistry of its synthetic equivalent spinel type (Cu, Fe) $(Re, Mo)_4S_8$, *Eur. J. Mineral.,* 1991, vol. 3, pp. 977–982.

Tolstykh, N.D., Krivenko, A.P., Krivolutskaya, N.A., Gongal'skii, B.I., Zhitova, L.M., and Kotel'nikova, M.V., *Blagorodnometall'naya mineralizatsiya v rassloennykh ul'trabazit-bazitovykh massivakh yuga Sibirskoi platform (Noble Metal Mineralization in Layered Ultramafic–Mafic Massifs of the Southern Siberian Platform)*, Novosibirsk: Parallel', 2008.

Vlasova, V.N., Sokol'nikova, Yu.V., Krasnoshchekova, T.S., Men'shikov, V.I., and Lozhkin, V.I., Determination of platinum group metals and gold in geological material by inductively coupled plasma mass spectrometry with separation of impediment elements by cation-exchane chromatography, *Problemy geokhimii endogennykh protsessov i okruzhayushchei sredy: Mater. Vseross. nauch. konf. (s mezhdunar. uchastiem)* (Geochemical Problems of Endogenous Processes and Environment Proceedings of All-Russian Scientific Conference (with International Participation), Irkutsk: Inst. Geografii im. V.B. Sochavy SO RAN, 2007, vol. 3, pp. 212–214.

Woodland, S.J., Pearson, D.G., and Thirlwall, M.F., A platinum group element and Re–Os isotope investigation of siderophile element recycling in subduction zones: comparison of Grenada, Lesser Antilles arc, and the Izu-Bonin arc, *J. Petrol.,* 2002, vol. 43, no. 1, pp. 171–198.

Yarmolyuk, V.V., Kovalenko, V.I., and Kuzmin, M.I., North Asian superplume activity in the Phanerozoic: magmatism and geodynamics, *Geotectonics,* 2000, vol. 34, no. 5, pp. 343–366.

Zavaritskii, A.N., *Izverzhennye gornye porody (Igneous Rocks)*, Moscow: Akad. Nauk SSSR, 1961.

Zolotukhin, V.V., Polyakov, G.V., Balykin, P.A., and Glotov, A.I., Genetic aspect of Cu–Ni sulfide mineralization during komatiite and related magmatism, *Russ. Geol. Geophys.,* 2001, vol. 42, no. 7, pp. 1090–1099.

Translated by I. Baksheev